Biomolecules and Biomedicine

ISSN: 2831-0896 (Print) | ISSN: 2831-090X (Online)
Journal Impact Factor® (2024): 2.2

CiteScore® (2024): 5.2
www.biomolbiomed.com | blog.bjbms.org

RESEARCH ARTICLE

Pećina-Šlaus et al: EMT markers in glioma

In silico analysis reveals distinct changes in markers of epithelial to mesenchymal transition in glioma subtypes

Nives Pećina-Šlaus[1,2#*], Alja Zottel[3#], Željko Škripek[1], Borna Puljko[4,5], Fran Dumančić[1,2], Anja Bukovac[1,2], Ivana Jovčevska[3], and Anja Kafka[1, 2]

[1]Department of Biology, School of Medicine, University of Zagreb, Zagreb, Croatia;

[2]Laboratory of Neuro-oncology, Croatian Institute for Brain Research, School of Medicine University of Zagreb, Zagreb, Croatia;

[3]Center for Functional Genomics and Biochips, Institute of Biochemistry and Molecular Genetics, Faculty of Medicine, University of Ljubljana, Ljubljana, Slovenia;

[4]Laboratory for molecular neurobiology and neurochemistry, Croatian Institute for Brain Research, School of Medicine, University of Zagreb, Zagreb, Croatia;

[5]Department of Chemistry and Biochemistry, School of Medicine, University of Zagreb, Zagreb, Croatia.

***Correspondence to** Nives Pećina-Šlaus: nina@mef.hr

#These authors equally contributed to this work.

DOI: https://doi.org/10.17305/bb.2025.12598

ABSTRACT

Epithelial to mesenchymal transition (EMT) plays a critical role in tumor progression and metastasis, including in gliomas. To examine and interpret data on major genes involved in EMT and associate their changes with low-grade (LGG) and/or high-grade (HGG) gliomas, data from the cBioPortal—a publicly available database for tumor genomics and transcriptomics, were collected for 13 genes: *CDH1, CDH2, CTNNB1, LEF1, NOTCH1, SNAI1, SNAI2, SOX2, TJP1/ZO1, TWIST1, VIM, ZEB1,* and *ZEB2*. The dataset included mutations, copy number alterations (CNA), and changes in transcript levels reported for each gene. The genes were additionally validated by gene expression on the GlioVis portal, STRING protein network analysis, survival analysis, and experimentally with qRT-PCR. Glioblastoma and diffuse glioma harbored changes in all 13 analyzed genes, while anaplastic oligodendroglioma and anaplastic astrocytoma in 46.15%, oligodendroglioma in 23.08%, and oligoastrocytoma in 15.38%. *NOTCH1* and *SOX2* were most affected by changes. The *NOTCH1* gene was statistically more frequently changed compared to *CDH1*, *CTNNB1,* and *ZEB1* ($p < 0.05$). The virtual study showed that alterations in *NOTCH1* and *LEF1* were associated with LGG, while alterations in *CDH1, CTNNB1, TJP1, TWIST1, SOX2*, *VIM, ZEB1,* and *ZEB2* were associated with HGG. Differential expression analysis stratified for *IDH1* mutations showed that *IDH1*-mutant glioblastoma had significantly lower *CDH2, LEF1* and *SNAI1* expression, and higher *ZEB1*. Gene expression in different glioblastoma subtypes showed that the *TJP1/ZO1* gene was associated with the classical subtype, while *ZEB2* was associated with the proneural subtype. qRT-PCR confirmed GlioVis mRNA expression data for *NOTCH1, SOX2, CDH1, CTNNB1, TJP1/ZO-1, VIM, TWIST1,* and partially for *SNAI1 (SNAIL), SNAI2,* and *CDH2.* Our study shows consistent changes in genes involved in EMT in gliomas of different grades. Additional research is needed to confirm the knowledge brought by this study.

Keywords: Glioma; EMT marker; *NOTCH1*; *SOX2*; progression; WHO grade; cBioPortal; GlioVis; qRT-PCR

INTRODUCTION

Epithelial-to-mesenchymal transition (EMT) is a molecular program by which a cell acquires migratory abilities. Cells lose epithelial characteristics and tissue integrity, and develop a mesenchymal phenotype [1, 2]. Besides its central role in embryonic development, EMT is also important for wound healing, tissue fibrosis, and tumorigenesis. In tumorigenesis, EMT is responsible for invasiveness and metastasis [3]. However, the binary phenotypes, epithelial and mesenchymal, cannot fully explain the real EMT phenomenon in clinical settings. As evidenced by several distinct molecular processes that are engaged, the concept of EMT can be regarded as a "spectrum" [4, 5]. Recent research has shown that there is a hybrid (partial) EMT state characterized with both mesenchymal and epithelial features and associated with increased cellular plasticity, collective migration, stemness properties and more pronounced metastatic potential [6, 7, 8]. To describe the involvement of epithelial and mesenchymal markers, as well as the activation of various EMT transcription factors (EMT–TFs) we focused on the following genes, all sharing important roles in the EMT: *CDH1, CDH2, TJP1/ZO-1, CTNNB1, LEF1, NOTCH1, SNAI1, SNAI2, SOX2, TWIST1, VIM, ZEB1* and *ZEB2*. Major markers of the epithelial phenotype are E-cadherin, encoded by the *CDH1* gene, and tight junction protein-1 encoded by *TJP1/ZO-1* gene (TJP1, *Zonula occludens-1*, ZO-1). The marker of mesenchymal phenotype is primarily N-cadherin encoded by the *CDH2* gene [9], followed by vimentin, encoded by *VIM*, beta-catenin (gene *CTNNB1*), Lymphoid Enhancer Binding Factor 1 (*LEF1*) and *NOTCH1*. Additional genes coding for EMT-related transcription factors (EMT–TFs) were also included in the study, *SOX2, TWIST1, SNAI1, SNAI2, ZEB1* and *ZEB2*. EMT also plays a role in glioma tumors.

Gliomas are one of the most common intracranial tumors with great aggressiveness and invasiveness. An important reason for the high invasion of glioma cells is the acquisition of mesenchymal properties with the ability to invade and migrate [1, 10]. Gliomas, primary tumors of the central nervous system (CNS), arise from glial cells. Now all gliomas are grouped into one category based on mitotic activity, diffuse growth pattern, and the mutational status of the *IDH1* and *IDH2* genes, together with several other molecular biomarker tests. According to the World Health Organization (WHO) [11-13] tumors are divided into four grades. Tumors are graded within tumor types rather than across different types [13]. The prognosis of diffuse glioma depends on several factors including tumor grade. Grades that were recorded on cBioPotral and included in our analysis were: diffuse gliomas (grade 2), oligodendrogliomas (grade 2), oligoastrocytomas (grade 2), anaplastic

oligodendroglioma (grade 3), anaplastic astrocytoma (grade 3), and glioblastoma (grade 4). Gliomas can also be grouped into low grade gliomas (LGG includes grades 1 and 2) and high-grade gliomas (HGG includes grades 3 and 4). LGGs are brain tumors that mostly affect young adults. They grow more slowly and are associated with a more favorable prognosis compared to high grade gliomas (HGG).

Data from several studies available in the cBioPortal public database were analyzed *in silico*. Molecular markers of EMT were compared between the LGG and HGG groups. We hypothesized that specific changes in genes encoding mesenchymal phenotype markers are associated with higher glioma grades, while changes in epithelial marker genes with lower ones. We collected data on mutations, amplifications and deletions, and analyzed the specific type and frequency of changes for each selected gene. The observed changes reported in cBioPortal were validated by additional database search and qRT-PCR. We also performed *in silico* analysis of gene expression across different glioma grades, survival analysis as well as protein network analysis.

MATERIALS AND METHODS

cBioPortal

The analysis of selected genes in gliomas of different pathohistological types and grades was performed using data in The cBioPortal for Cancer Genomics database [14, 15]. The analyses included stored data on mutations, copy number alteration (CNA), and the expression of mRNA.

Analyzed studies

Eight studies from the cBioPortal database were included, which contained 3497 samples, obtained from 3143 patients. Collective studies had queried genes altered in 379 (12%) of queried patients and 395 (11%) of queried samples. Selected studies were: *Diffuse Glioma* (GLASS Consortium, Nature 2019) [16]- whole genome or whole exome sequencing analysis of 444 adult patients; *Glioma* (MSK, Clin Cancer Res 2019) [17]- targeted sequencing on MSK-IMPACT and FMI Panels of 1004 samples; *Low-Grade Gliomas* (UCSF, Science 2014) [18]- whole exome sequencing of 61 samples; *Merged Cohort of LGG and GBM* (TCGA, Cell 2016) [19]- whole exome sequencing of 1.122 LGG and GBM tumor/normal pairs; *Brain Tumor patient-derived xenografts* (PDXs) (Mayo Clinic, Clin Cancer Res 2020) [20] - whole exome sequencing on a total of 106 samples; *Glioblastoma* (CPTAC, Cell 2021) [21] - proteogenomic and metabolomic characterization of human glioblastoma and whole

genome or whole exome sequencing of 99 samples generated by CPTAC; *Glioblastoma* (Columbia, Nat Med. 2019) [22]- whole-exome sequencing of 42 glioblastomas samples with matched normals and *Glioblastoma Multiforme* (TCGA, Firehose Legacy) 619 samples – source data from GDAC Firehose previously known as TCGA Provisional [14, 15]. Data on mutations, changes in the number of copies (CNA - *copy number alteration*) and transcript levels (mRNA) of each gene were downloaded and examined as a classic study. All cBioPortal data have the same clinical criteria and equally processed and normalized data, which enables comparative analysis of samples between different studies. After creating a virtual study, graphical representations of gene analysis were made in Excel 2016 (Microsoft). Our virtual study, done in March 2025, has downloadable data available at [23]. The current version of the human genome that cBioPortal uses as a reference is hg19/GRCh37. Portal RNA and DNA data were obtained from tumor samples and adjacent normal tissue using an adaptation of the DNA/RNA AllPrep kit (QIAGEN). Pathologists systematically reviewed the specimens to confirm the histopathological diagnosis applying the criteria of the latest edition of the WHO classification for each tumor type. Copy number data were generated on Affymetrix SNP 6.0 arrays using standard protocols from the Broad Institute Genome Analysis Platform. CNAs are continuous gene copy number values obtained as the difference between the copy number of the tumor gene and the reference. Normalized continuous CNA values were processed using the copy-number analysis algorithm *Genomic Identification of Significant Targets in Cancer* (GISTIC 2.0) indicating the copy-number level per gene. Continuous values -2 were listed as deep deletions that indicates a deep loss, a homozygous deletion. Values -1 or shallow deletion indicates a shallow loss, a heterozygous deletion. Samples whose continuous CNA value was 0 were declared as diploid samples with no gene copy number changes. Value 1 or gain indicates a low-level gain (a few additional copies, often broad), while amplifications are characterized with value 2 indicating high-level amplification (more copies, often focal).

The cBioPortal ensures comparability across datasets. Data from the PanCancer Atlas is divided by tumor type, but these studies have uniform clinical elements, consistent processing and normalization of mutations, copy number, mRNA data and are ideally processed for comparative analyses.

All samples were statistically processed according to the following variables: pathohistological diagnosis, frequency, and type of changes (mutation, CNA), malignancy grade. Statistical analysis was performed using IBM SPSS Statistics 23.0 software (SPSS,

Chicago, IL, USA) with a significance of $p < 0.05$. Gene alterations were analyzed in specific tumor types using the Fisher's exact test. Correction for multiple comparisons was adjusted with Benjamini–Hochberg False Discovery Rate (FDR) method.

Gene expression in different glioma grades

Gene expression analysis across different glioma grades (WHO grade 2, 3, and 4) was performed using the GlioVis online tool, including the TCGA_GBMLGG dataset (https://gliovis.bioinfo.cnio.es/). To assess expression differences among different glioma types as well as glioblastoma subtypes, a one-way Analysis of Variance (ANOVA) was performed independently for each gene. A Tukey's Honest Significant Difference (HSD) test was used to perform post hoc comparisons between groups [24]. To quantify the strength of subtype effects, η^2 (eta squared) effect sizes were calculated from the ANOVA models. To correct for multiple testing across all genes, ANOVA p-values were adjusted using the Benjamini–Hochberg False Discovery Rate (FDR) method. Additionally, FDR correction was applied across all pairwise comparisons from the Tukey HSD tests.

Gene expression in glioblastoma

The *Glioblastoma Multiforme* study (TCGA, Firehose Legacy) was used for mRNA expression analysis, which included data available for 619 samples.

For mRNA expression level data, next-generation RNASeq V2 RSEM (*RNA-seq by Experimentation Maximization*) sequencing was downloaded. [25]. RNASeqV2 from TCGA is processed and normalized using software RSEM. Specifically, the RNASeq V2 data in cBioPortal corresponds to the rsem.genes.normalized_results file from TCGA. A more detailed explanation of RSEM output can be found at https://www.biostars.org/p/106127/. cBioPortal then calculates z-scores. The expression data assigned from Illumina were batch-corrected to correct platform variations between the GAII and HiSeq Illumina sequencers. Additional corrections were made for various sequencing centers [26]. More precisely, the RNASeq V2 data in cBioPortal matches *the rsem.genes.normalized_results* file from TCGA. cBioPortal mRNA expression data are calculated as relative expression of a specific gene in a tumor sample to the gene's expression distribution in a reference (all samples that are diploid for the gene in question) population of samples [15].

During the data normalization process, expression data (RPPA) for protein were batch effects-corrected and median-centered in both directions. Within cBioPortal, the protein data

were additionally processed and normalized with the calculation of the z-scores and converted on the log scale.

Differential analyses stratified according to *IDH1* status and glioma subtypes

Differential expression analysis was performed on TCGA_GBMLGG dataset (obtained from Gliovis [24]), stratified for Grade 2, Grade 3, GBM (glioblastoma) *IDH1* wt (wild type) and GBM *IDH1* mut (mutated).

Subtypes analysis was also on GlioVis TCGA_GBMLGG dataset, filtered for GBM *IDH1* wt only. Both analyses were performed using R (4.4.0) and RStudio (2023.06.0). Statistical significance was determined by One-way anova statistical test.

Validation by qRT-PCR

Glioma samples graded from 2 to 4 were collected from the University Hospital Center "Zagreb", University Hospital Center „Sestre Milosrdnice", Zagreb and University Medical Centre Ljubljana. Certified neuropathologists set the accurate diagnosis in concordance with the most recent WHO classification [12]. The patients included in the study had no family history of brain tumors and did not undergo any cancer treatment, prior to surgery, which could affect the results of qRT-PCR analyses. Altogether there were 18 samples grade 2 (LGG) of which 17 were *IDH1* mutant and one was wild type (mean age = 40.22). HGG gliomas consisted of 5 samples grade 3 of which 4 were *IDH1* mutant and one was wild type. Sixteen samples were grade 4 (glioblastoma, GBM) of which two were *IDH1* mutant and 12 were wild type (two samples were not determined for *IDH1*). Mean age of HGG patients was 55.7 years. Furthermore, 12 non-tumor reference brain tissues were collected as qRT-PCR controls.

Quantitative real-time polymerase chain reaction (qRT-PCR) was performed to validate the candidate genes. Experimental validation by qRT-PCR was performed on normal brain tissues, LGG and HGG tissue samples. The GeneJET RNA Purification kit (Thermo Fisher Scientific #K0702) was used to extract total RNA from brain tissue samples from both healthy and tumorous subjects, while some of the RNA was already isolated as described in [27]. The High-Capacity cDNA Reverse Transcription Kit with RNase Inhibitor (Applied Biosystems #4388950) was used to reverse-transcribe equal amounts of RNA after it had been treated with DNase I (Sigma-Aldrich #EN0521). Each sample was subjected to qRT-PCR analysis using a constant quantity of cDNA using the qRT-PCR SYBR Green PCR (Applied Biosystems, #4309155) or TaqMan fast Advanced Mastermix (Thermofisher,

#4444557) based qRT-PCR. Supplementary Table S1 lists the primer sequences that were employed. The relative quantification approach (ΔΔCt) was utilized to determine the target gene expression for group comparisons normalized per beta-actin as an endogenous control. To determine the target gene expression for group comparisons, a 7900 HT Real-Time PCR System (Applied Biosystems) or QuantStudio 7 Pro (ThermoFisher) was utilized for real-time fluorescence detection.

qRT-PCR validation of SOX2 and NOTCH1

For *SOX2* and *NOTCH1* validation, RNA had been previously extracted as described in earlier studies [27]. For each sample, 500 ng of total RNA was treated with DNase I (Roche) at 30 °C for 15 minutes, followed by enzyme inactivation at 75 °C for 10 minutes. cDNA was synthesized using the High-Capacity cDNA Reverse Transcription Kit (Thermo Fisher Scientific), with the addition of RNase inhibitor (1 µL per reaction; Cat. No. N8080119, Thermo Fisher). The reverse transcription protocol was carried out under the following conditions: 10 minutes at 25 °C, 120 minutes at 37 °C, and 5 minutes at 85 °C. qRT-PCR was performed using TaqMan assays in a 5 µL reaction volume, containing 0.25 µL of the TaqMan gene expression assay, 2.5 µL of TaqMan Gene Expression Master Mix, 2 µL of nuclease-free water, and 0.25 µL of diluted cDNA. Thermal cycling was carried out under the following conditions: 95 °C for 20 seconds for initial denaturation, followed by 45 cycles of 95 °C for 1 second and 60 °C for 20 seconds, with a final hold at 4 °C. All reactions were run in technical triplicates. The probes used in the study were following: GAPDH Hs99999905_m1, HPRT1Hs02800695_m1, SOX2 Hs04234836_s1, NOTCH1 Hs01062014_m1 (all from ThermoFisher). Data was analyzed according to MIQE guidelines [28].qRT-PCR data is shown as X ± SEM. Data was analyzed as described before [29]. First, data was checked for normality using Shapiro-Wilk test. As data did not follow normal distribution, non-parametric Kruskal-Wallis test with Dunn's multiple comparisons test was applied. A significance threshold was set at 0.05. GraphPad Prism version 9 was used to process and display all of the data graphically (GraphPad Software Inc.).

Survival analyses

We performed age adjusted survival analysis for samples that were *IDH1* wild type (wt) and those that carried *IDH1* mutations. Survival analysis was conducted on the TCGA_GBMLGG dataset obtained from GlioVis [24], separately for GBM *IDH1* wild-type and GBM *IDH1* mutant samples. Patients were stratified into high and low expression groups for each gene based on median expression. Kaplan–Meier curves were generated and

compared using the log-rank test. Multivariate Cox proportional hazards models were used to estimate hazard ratios (HRs) and 95% confidence intervals (CIs), adjusting for age. All analyses were performed in R (v4.4.0) using RStudio (2023.06.0) with the survival and survminer packages.

Protein network analysis

Protein network analysis was performed by the STRING online tool [30]. The following genes were included into the analysis: *CDH1, CDH2, TJP1/ZO-1, CTNNB1, LEF1, NOTCH1, SNAI1, SNAI2, SOX2, TWIST1, VIM, ZEB1, ZEB2*. The interaction score was set to 0.9 (highest confidence) [31].

Ethical statement

The Ethics Committees of the School of Medicine, University of Zagreb (Case number: 380-59-10106-20-111/126; Class: 641-01/20-02/01), University Hospital Center Zagreb (Case number: 02/21 AG; Class: 8.1-20/108-2), and University Hospital Center „Sestre Milosrdnice“ (Case number: 251-29-11-20-01-9; Class: 003-06/20-03/015)have approved the research. The use of human tissue samples was approved by the National Medical Ethics Committee of the Republic of Slovenia (Approval Numbers: 92/06/12, 89/04/13, and 95/09/15). Reference samples were collected during autopsies in accordance with the legal regulations of the Republic of Slovenia. All samples used in this study are anonymized. The study adhered to the principles outlined in the Declaration of Helsinki with patients consent to participate.

Data retrieved from the publicly available cBioPortal database do not require ethical approval. All patients whose samples were used in this analysis signed an informed consent. Since the data are not identifiable secondary data analysis does not require additional ethical approval since it was already obtained at original analyses [16-22]. The secondary data analysis was performed in compliance with the World Medical Association Declaration of Helsinki on Ethical Principles for Medical Research Involving Human Subjects. The data is properly anonymized making it impossible to identify individuals.

Pathway enrichment analysis

To explore how these genes interact within EMT pathways, enrichment analysis was performed to indicate pathways where the selected EMT genes are involved. The genes were analyzed with NDEx online tool (https://cytoscape.org/).

RESULTS

The overview of genetic changes distributed to glioma type

Our first analysis summarized all genetic changes reported for gliomas. Table 1 provides an overview of a pooled analysis that eight studies found in 13 genes involved in EMT in low- and high-grade gliomas (LGG and HGG). Mutations prevailed over amplifications and deep deletions, while a small number of gliomas harbored multiple changes. Anaplastic oligodendrogliomas (grade 3) contained the highest percentage of mutations, 29.03% (18/62 cases), and oligodendrogliomas followed with 16.79%. Anaplastic astrocytomas harbored 7.58%, oligoastrocytomas 6.25%, while mutations in glioblastoma were present in 5.91% (98/1659 cases) and diffuse glioma in 4.91%. Although the percent of amplifications for oligoastrocytomas was high 6.25% (1/16 cases), this frequency should be taken with caution since only 16 samples were available. However, when other grade 2 glioma subtype is observed, diffuse gliomas at 4.91% (65/1324 cases), it was shown that amplifications were associated with grade 2 gliomas. Deep deletions were found in 0.54% of glioblastomas and in 0.98% of diffuse gliomas. Multiple changes were reported in 0.23% of diffuse gliomas, and 0.12% of glioblastoma cases.

Changes in the *CDH1* and *CDH2* genes

Mutations were a predominant type of change for *CDH1* gene, and only one case of glioblastoma (0.06%) harbored deep deletion. *CDH1* was most often mutated in oligodendrogliomas, 2.19% (3/137 cases), and glioblastomas followed with 1.69% (28 cases). As the grade of glioma decreased, so did the number of cases in which *CDH1* was mutated, thus anaplastic oligodendroglioma harbored 1.16% and anaplastic astrocytoma 1.01%. The lowest number of mutations were present in diffuse gliomas (grade 2) with only 0.38% (5/1324 cases) (Figure 1). Seven mutations were characterized as drivers and oncogenic. The results of the *CDH2* gene analysis were somewhat reciprocal to those obtained for the *CDH1* gene (Figure 1). For instance, *CDH1* mutations predominated in oligodendroglioma and glioblastoma, while *CDH2* mutations were not reported for oligodendroglioma. Mutations were present in only 0.24% and 0.17% of glioblastoma and diffuse glioma, respectively. *CDH2* was mutated most frequently (4.08%) in anaplastic astrocytoma (grade 3). Mutations were of unknown significance and none was characterized as oncogenic. Contrary to *CDH1*, where no amplifications were found, amplifications of *CDH2* were present in a small percentage of diffuse gliomas and glioblastoma, 0.25% and 0.24%,

respectively. Deep deletions of the *CDH2* were also recorded in these two types, in diffuse glioma in 0.17%, and glioblastoma in 0.12% (Figure 1).

TJP1/ZO-1 gene changes

The gene for the tight junction adapter protein, *TJP1/ZO-1*, was mutated, amplified, and deeply deleted. Again, mutations were the most common change. Thirty different mutations were all of the unknown significance. They were most pronounced in anaplastic oligodendroglioma (grade 3) with 6.25%. Altogether the *TJP1/ZO-1* gene was mutated in 1.43% (16 cases), amplified in 1 case (0.09%), and deeply deleted in 0.27% (3 cases) of glioblastomas (Figure 1). Diffuse gliomas harbored 0.71% of mutations, 0.09% of amplifications and 0.27% of deep deletions (Figure 1).

CTNNB1 gene changes

Predominant alterations of *CTNNB1* were mutations. Of 26 mutations reported one was an oncogenic driver, and the rest were of unknown significance. They were found in 1.61% of anaplastic oligodendroglioma, 1.01% of anaplastic astrocytoma, 0.90% of glioblastoma and 0.44% of diffuse glioma. The results obtained for the *CTNNB1* gene show that the changes were most frequently confined to grade 3 gliomas (Figure 1). Deep deletions were reported for glioblastoma and diffuse glioma, 0.12% and 0.35%, respectively. Only one diffuse glioma (grade 2) (0.09%) harbored amplification of *CTNNB1* (Figure 1).

LEF1 gene changes

The changes in the *LEF1* gene were confined to diffuse glioma and glioblastoma. Both mutations and amplifications were more frequent in diffuse glioma compared to glioblastoma. Mutations of unknown significance were present in 0.27% of diffuse glioma versus 0.18% in glioblastoma. Amplifications in diffuse glioma (grade 2) amounted to 0.27%, compared to 0.09% found in glioblastoma. There was also one diffuse glioma (0.09%) with deep deletion of this gene (Figure 1).

VIM gene changes

Changes in the *VIM* gene (vimentin), including mutations, amplifications and deep deletions, were differently distributed in patients with glioblastoma compared to diffuse gliomas. In glioblastoma the gene was mutated in 0.45% (5/1120 cases), amplified in 0.09% (1 case), and deleted in one case (0.09%). On the other hand, in diffuse gliomas (grade 2) it was amplified (0.53%; 6/1131 cases) more often than mutated (0.09%). The mutations were of unknown significance (Figure 1).

NOTCH1 gene changes

NOTCH1 gene showed a high percent of changes across all types of gliomas. The obtained results indicated that the prevalent type of changes were mutations, while amplifications and deep deletions were extremely rare. There were 193 mutations of which 72 were characterized as oncogenic drivers. The largest number of mutations was registered in anaplastic oligodendroglioma (grade 3) in 27.42% (17 cases), followed by mutations in oligodendroglioma (14.60%), oligoastrocytoma (6.25%), anaplastic astrocytoma (5.05%), and diffuse gliomas (3.1%). Glioblastomas harbored mutations in 3.13% (52/1659 cases), while amplifications were present in 0.42% (7/1659 cases). Diffuse gliomas also harbored amplifications in 0.76% and deep deletions in 0.15% (Figure 1).

SNAI1 and *SNAI2* genes changes

Interesting results were obtained for the *SNAI1* gene that was changed only in diffuse glioma and glioblastoma. Namely, unlike previous genes where mutations prevailed, here amplifications were the most common changes. They were more frequent in glioblastoma compared to diffuse gliomas. *SNAI1* gene amplification in glioblastomas occurs in 0.24% (2 cases), and in diffuse gliomas in 0.18% (2 cases) Mutations in diffuse glioma were recorded in only 0.09% and were not characterized as oncogenic (Figure 1). The next gene included in the analysis is the transcriptional repressor *SNAI2*. Similar to *LEF1* and *SNAI1*, changes in this gene have been reported only in glioblastoma and diffuse gliomas. However, unlike *SNAI1*, where amplifications predominated, here mutations were most common. The gene was more often mutated in glioblastoma compared to diffuse gliomas, in 0.27% (3/1120 cases) versus 0.18% (2/1131 cases). Only 0.09% of diffuse gliomas showed amplification. In contrast to *SNAI1,* is the presence of deep deletions of *SNAI2* in both glioblastoma (0.09%) and diffuse glioma (0.09%) (Figure 1).

TWIST1 gene changes

TWIST1 changes were more frequent in glioblastoma compared to diffuse glioma. Amplifications prevailed over mutations. In diffuse gliomas (grade 2), the gene was amplified in 0.42% and mutated in 0.08%. In glioblastoma, the gene was amplified in 0.63% and mutated in 0.36% of samples (Figure 1.)

SOX2 gene changes

The results of the analysis of the *SOX2* gene were similar to the *SNAI1* gene, with respect that both genes were most frequently amplified. The highest number of amplifications was found

in 6.25% of oligoastrocytomas (grade 2) and 4.04% (8 cases) of anaplastic astrocytomas (grade 3). Anaplastic oligodendroglioma harbored amplifications in 3.23% and oligodendroglioma in 2.92%, while in glioblastoma they were present in 2.9% of cases and diffuse glioma in 2.42%. *SOX2* mutations were present in 1.52% of anaplastic astrocytoma, 0.54% of glioblastoma, and 0.076% of diffuse glioma. One case (0.06%) of glioblastoma showed multiple *SOX2* gene changes (Figure 1). Missense mutations of unknown significance predominated.

ZEB1 and *ZEB2* gene changes

The highest percent of *ZEB1* mutations (6.25%) was associated with anaplastic oligodendrogliomas (grade 3). Anaplastic astrocytoma (grade 3) followed with 2.56% and glioblastoma with 0.89%, while diffuse gliomas had 0.18%. All of the mutations are of unknown significance. In addition to mutations, glioblastomas and diffuse gliomas also harbored amplifications (0.18% and 0.53%). Deep deletion of the *ZEB1* gene was present in one diffuse glioma (0.09%) (Figure 1).

The last gene included in the analysis was *ZEB2*. Unlike *ZEB1*, where glioblastoma ranked third in terms of the frequency of gene changes, here it ranked first. Mutations prevailed in glioblastomas in 0.89%, while amplifications were present in 0.18%, and deep deletions in 0.09%. Changes of *ZEB2* in diffuse gliomas (grade 2) were less frequent. The gene was mutated in 0.44%, amplified in one case (0.09%), and deeply deleted also in one case (Figure 1).

Collective results of genetic changes distributed to LGG and HGG

To illustrate all the changes associated with each gene and divide them into low- and high-grade glioma groups, we made a summary in Figure 2. From the figure, it is evident that in both groups of gliomas, the *NOTCH1* and *SOX2* genes were most affected by changes. *CDH1, CTNNB1, TJP1/ZO-1, ZEB1,* and *ZEB2* mutations were more common in high-grade gliomas. Only glioblastoma and diffuse glioma had changes in all 13 analyzed genes. Anaplastic oligodendroglioma and anaplastic astrocytoma harbored changes in 6/13 (46.15%), oligodendroglioma in 3/13 (23.08%), and oligoastrocytoma in 2/13 (15.38 %) of the analyzed genes. In less than half (6/13 or 46%) of the analyzed genes, changes were distributed only in glioblastoma and diffuse glioma. In 7 analyzed genes: *CDH1, CDH2, CTNNB1, NOTCH1, SOX2, TJP1/ZO-1* and *ZEB1*, changes were present in several pathohistological diagnoses ranging from 3 to all 6. Genes in which changes were present in

all 6 pathohistological diagnoses were *NOTCH1* and *SOX2*. Changes of the *CDH1* gene were present in 5/6 glioma types, of *CTNNB1* and *ZEB1* genes, in 4/6 pathohistological types, and of *CDH2* and *TJP1/ZO-1*, in 3/6 glioma types. Regarding the genes whose changes were associated with any of these 6 pathohistological types, *NOTCH1* and *SOX2* changes were present in all glioma types. Furthermore, the frequency of changes in those genes where changes were present was statistically significantly higher in the *NOTCH1* gene than in the *CDH1* gene in anaplastic oligodendroglioma (Benjamini-Hochberg Adjusted P value, significant using an FDR of 0.05 ($P<0.05$), oligodendroglioma ($P<0.05$), glioblastoma ($P<0.05$), anaplastic astrocytoma ($P<0.05$) and diffuse glioma ($P<0.05$). The same trend was present when the frequency of changes in the *NOTCH1* was compared with that of the *CTNNB1* gene - the frequency of changes in the *NOTCH1* was significantly higher in anaplastic oligodendroglioma ($P<0.05$), glioblastoma ($P<0.05$), anaplastic astrocytoma ($P<0.05$) and diffuse glioma ($P<0.05$). A comparison of the frequency of changes in the *NOTCH1* gene and the *ZEB1* gene shows that the frequency of changes in the *NOTCH1* gene was significantly higher in glioblastoma ($P<0.05$) and diffuse glioma ($P<0.05$). However, in anaplastic oligodendroglioma and anaplastic astrocytoma, the frequency of changes in these two genes was similar.

Gene expression in different glioma grades

In the next part, we analyzed the gene expression *in silico* (results obtained from GlioVis, TCGA_GBMLGG dataset included). From the results, we can observe that *CDH2*, *CTNNB1*, *VIM*, *LEF1*, *TWIST1*, *SNAI1,* and *SNAI2* are overexpressed in glioblastoma (grade 4) versus gliomas grade 3 and 2. *NOTCH1*, *SOX2*, *TJP1/ZO1*, *ZEB1* and *ZEB2* have higher expression in lower-grade glioma versus glioblastoma (Figure 3)

Gene expression in glioblastoma

mRNA expression analysis on samples from The *Glioblastoma Multiforme* study (TCGA, Firehose Legacy) was obtained by next-generation sequencing from RNASeq V2 RSEM, downloaded from cBioPortal and shown in Figure 4.

A higher level of mRNA expression was noted for the majority of queried genes: *TWIST1, CTNNB1, SNAI1, NOTCH1, ZEB2, SNAI2, CDH1, CDH2*, and *LEF1,* while gene *TJP1/ZO-1* showed a reduced level of mRNA transcript. For the *SOX2*, similar number of samples had elevated mRNA levels as well as decreased. The Figure 4. also shows high/low protein expression for several genes.

We also investigated post-transcriptional events, by analyzing methylation patterns. We inspected cBioPortal and found that mRNA expression levels were associated to levels of methylation for genes *CDH1* (Spearman: -0.27; P=0.0209), *NOTCH1* (Spearman: -0.22; P=0.0619), *TJP1/ZO-1* (Spearman: -0.27; P=0.0174), *SNAI1* (Pearson:-0.30; P=0.0174), *SNAI2* (Pearson: 0.28; P=0.0251), *VIM* (Spearman: 0.25; P=0.0496).

Differential analysis stratified according to *IDH1* status

The results of differential expression analysis performed on TCGA_GBMLGG in grade 2, grade 3 and grade 4 (GBM) stratified according to *IDH1* wt and *IDH1* mutations, indicated similar results that were obtained without this stratification (Figure 5). However, when we divided samples, for *IDH1* wt/mut it was demonstrated that genes *CDH2, LEF1, SNAI1* and *ZEB1* showed significant expression differences between *IDH1* wt and *IDH1* mutant glioblastoma. *CDH2*, *LEF1* and *SNAI1* had lower expression in *IDH1* mutant samples, while *ZEB1* had significantly higher expression levels in samples harboring *IDH1* mutations (Figure 5).

Glioblastoma subtypes analysis

The results of differential expression in different glioblastoma subtypes, classical, mesenchymal, proneural and neural, clearly showed that *TJP1/ZO-1* gene was associated with classical subtype, while *ZEB2* with proneural subtype (Figure 6).

qRT-PCR validation

We performed qRT-PCR for all selected genes in HGG, LGG, and normal brain tissues. Except for *LEF1*, *NOTCH1* and *SOX2*, there was no statistical significance observed in the upregulation or downregulation of the candidate genes. However, the expression levels differed. The levels of *CDH1, LEF1,* and *TJP1/ZO-1,* were lower in both LGG and HGG in comparison to normal controls. *CTNNB1*, *TWIST1, VIM, ZEB1*, and *ZEB2* had higher levels in HGG than LGG, while *SOX2*, *NOTCH1, SNAI1, SNAI2* and *CDH2*, had higher levels in LGG than HGG (Figure 7A,B). When comparing our qRT-PCR results to both databases, we have observed that expressions were compatible for the majority of genes (Table 2). *CTNNB1* rose in higher grades which was compatible with data from GlioVis. Both *NOTCH1* and *SOX2* expression fell in higher grades which was compatible with GlioVis, and cBioPortal. *TJP1/ZO-1* was low in both groups, lower than controls and this was in accordance with both cBioPortal and GlioVis and biologically logical. *VIM* and *TWIST1* qRT-PCR levels were concordant with both GlioVis and cBioPortal. qRT-PCR data were partially compatible for

SNAI1, SNAI2, and *CDH2* for showing higher levels in LGG, but discordant with GlioVis for lower levels in HGG. However, both *ZEB1* and *ZEB2* were rising in higher grades showing higher levels of expression than controls which was different from GlioVis. However, *ZEB2* was compatible with glioblastoma high expression reported in cBioPortal. *LEF1* was also not compatible to databases. qRT-PCR showed *CDH1* levels lower than controls, which is biologically logical. *CDH1* did not show difference between LGG and HGG which was compatible with GlioVis (Table S2 shows representative raw Ct values).

Survival analyses

In the last part, we aimed to analyze the relationship between gene expression and glioblastoma patient survival. From the results we can observe, that no gene except *TWIST1* is related to survival, while the higher expression of *TWIST1* is related to shorter overall survival (p=0.018). Age adjusted survival analysis showed that in *IDH1* wt glioblastomas no gene was associated with worse or better survival with p lower than 0.05. *TWIST1* had p value of 0.079. while *CTNNB1* p=0.063. (Figure 8A). For glioblastomas that were *IDH1* mutated again no gene was associated with worse or better survival. *TWIST1* again almost reached value of p=0.074. (Figure 8B) (Table 3). The limitation of the survival analyses is that they were not supplemented with outcome modifiers such as treatment variables that may co-vary with gene expression. However, MGMT methylation status was provided in the raw data and we have performed survival analysis of glioblastoma *IDH1* wt adjusted for MGMT methylation status. No gene was associated with worse or better survival.

Protein network analysis

A network of NOTCH1 and SOX2 was constructed using the STRING tool showing confidence in the connection. No other interactors were included in the network. The highest confidence (0.9) was applied. From the Figure 9, it is obvious that there is a strong inter-connection between different EMT genes.

Enriched pathways

Enrichment analysis indicated pathways where the selected EMT genes are interconnected. The pathways include: WP4239 (Epithelial to mesenchymal transition in colorectal cancer), WP5097 (CCL18 signaling that led to EMT or migration and invasion) and WP5469 (Hallmark of cancer: metastasis and epithelial-to-mesenchymal transition) (Figure S1).

DISCUSSION

Transcriptional program switching between epithelial and mesenchymal phenotypes is induced by multiple factors and signaling pathways [32, 33]. A present investigation of genes involved in EMT showed that the frequency and type of their changes were different across human glioma types. The investigation *in silico* included 3143 patients with glial tumors of various malignancy grades from cBioPortal, a public database for interactive exploration of multidimensional datasets in cancer genomics. cBioPortal provides high-quality access to molecular profiles and clinical parameters collected from large-scale cancer genomics projects and experimental studies. This database enables large-scale data processing, statistical analysis, and a graphical overview of changes observed in human tumors from the gene to the protein level.

The first among queried genes was the primary marker of the epithelial phenotype, E-cadherin, encoded by the *CDH1* gene. This transmembrane glycoprotein is localized in adherens junctions [34]. Reduced expression of E-cadherin is considered one of the main molecular events responsible for EMT [35]. In tumors, it has been assigned the role of a tumor suppressor, whose loss is particularly involved in the mechanisms of invasiveness [36, 37]. Schwechheimer et al. [38] reported on the lack of E-cadherin expression in both, astrocytomas, glioblastomas, and oligodendrogliomas, which is in accordance to the reports on frequent promoter hypermethylation of this gene. The results of our study showed frequent mutations of *CDH1* associated with higher malignancy grades out of which seven were characterized as oncogenic, suggesting the rise of invasive potential in more malignant tumors. Another investigated marker of epithelial phenotype was *TJP1/ZO-1* (TJP1, *Zonula occludens-1*, ZO-1), also known as tight junction protein-1. It encodes a 220 kDa cell membrane protein which acts as a tight junction adapter between the membrane and the actin cytoskeleton [39]. Mutations were also the most common change for *TJP1/ZO-1*. Higher grades also harbored more mutations as compared to lower ones. The expression levels of *CDH1* were a bit lower in higher grades while the *TJP1/ZO-1* transcript was significantly lower in higher grades according to GlioVis. qRT-PCR showed that *CDH1* and *TJP1/ZO-1* levels were lower than controls indicating reduced epithelial phenotype of higher-grade glioma. One of the most important markers of mesenchymal phenotype is N-cadherin encoded by the *CDH2* gene [9]. The protein plays a major role in the formation of nervous tissues, but in tumors, N-cadherin enhances the ability of cells to migrate and invade surrounding tissues [40, 41]. We have shown that the *CDH2* was most often mutated in

anaplastic astrocytoma (grade 3, 4.08%), while amplifications were present in a smaller percentage of diffuse gliomas and glioblastoma in which deep deletions were also recorded. Chen et al. [42] showed that N-cadherin may serve as a prognostic indicator for overall survival in patients with glioma. By studying The Cancer Genome Atlas (TCGA), Chinese Glioma Genome Atlas (CGGA), and Rembrandt databases, *CDH2* expression was identified as significantly higher in grade 4 than in grades 2 ($P<0.001$) or 3 ($P<0.001$) [43]. Our investigation showed that mRNA expression levels were significantly different between grades 2 and 4, 3 and 4, and 2 and 3, according to GlioVis, TCGA_GBMLGG. The rise in expression was significantly associated with higher grades, which corroborates the above-mentioned studies. New research shows that there is an abundant expression of the precursor of N-cadherin - proN-cadherin in the cell membrane of most examined gliomas [43].

NOTCH1 and *SOX2* were genes mostly affected by changes in both LGG and HGG. It has been recognized that both SOX2 and NOTCH1 are molecules essential for invasiveness and metastasis. *NOTCH1* is one of the four genes encoding a member of the NOTCH family of signaling receptors [44, 45]. NOTCH1 is upregulated in malignant tumors, has a central function in progression, and has been shown to promote EMT through Notch ligands named Jagged [46-48]. A highly active Notch signal is observed in glioma stem cells (GSCs) [49, 50]. Furthermore, the low overall survival has been attributed to NOTCH1 overexpression. Although studies have shown that NOTCH1 helps to induce EMT in both healthy and neoplastic cells, its role as a marker of the mesenchymal phenotype is still controversial, especially in gliomas, where *NOTCH1* has not yet been elucidated from the aspect of its role in EMT.

The transcription factor SOX2 (*SRY-Box Transcription Factor 2*) is associated with the late stages of EMT. Its intronless gene encodes a member of the high-mobility groupbox (HMG-box, SOX) family of transcription factors associated with SRY (Sex Determining Region-Y) [51, 52]. The *SOX2* gene product is required for the maintenance of stem cells in the CNS. Guetta-Terrier et al. [53] showed that SOX2 was up-regulated to reduce the methylation level of the *NOTCH1* promoter and enhance its expression in GSCs [33]. The expression levels of NOTCH1 in glioblastoma were positively correlated with SOX2, and VIM [33] in their study.

Present investigation indicates that the prevalent type of changes for *NOTCH1* were mutations, while amplifications and deep deletions were rare. There were 193 mutations of

which 72 were characterized as oncogenic drivers. *SOX2,* on the other hand, was predominantly amplified. Survival analyses showed no correlation between *NOTCH1* and *SOX2* expression and survival of glioblastoma patients. However, the data from GlioVis, TCGA_GBMLGG showed that there was a significant difference in mRNA expression levels for both NOTCH1 and SOX2, where grade 4 had significantly lower expression levels as compared to grades 2 and 3. Experimental validation with qRT-PCR showed that both *NOTCH1* and *SOX2* expression levels were falling in higher grades, which confirmed *in silico* results from GlioVis and cBioPortal. A significant decrease in the expression of *NOTCH1* and *SOX2* between control tissue and LGG and HGG was established.
In their work, Song et al. [54] showed that CDH1/β-catenin and Notch-1/Akt signaling pathways are targeted in glioma. Several components of the Notch pathway including NOTCH1 are highly expressed at the invasive edges of tumors, and the same can be said for the EMT marker vimentin. Notch also regulates the transcription of ZEB, Snail, and Slug, which repress E-cadherin and induce vimentin expression. Here, we showed that the *NOTCH1* gene was highly mutated in both LGG and HGG gliomas, which may indicate that such alterations happen early and are constant throughout the stages of glioma progression.

Defective activation of the Wnt signaling pathway has been detected in various cancers, including glioma [55], and nuclear accumulation of β-catenin is positively correlated with metastasis and recurrence resulting in poor clinical outcomes [56] characterizing β-catenin as a marker of the mesenchymal phenotype. The protein is part of the complex that makes up adherent junctions, where it anchors the actin cytoskeleton [57]. In addition, beta-catenin is also the main signaling molecule of the Wnt pathway. Prior studies report on higher β-catenin and C-myc activity in relapsed glioma than in the primary tumor [58]. Our results on the *CTNNB1* gene (β-catenin) showed that mutations were specifically frequent in anaplastic gliomas. Also, the total mutational burden was higher in HGG. When querying its mRNA expression levels, they were significantly higher in grade 4 tumors compared to grades 2 and 3 which indicates that its excessive expression has oncogenic properties. qRT-PCR showed that *CTNNB1* rose in higher grades which was compatible with data from GlioVis. Beta-catenin's partner in transcription regulation of the Wnt signaling is LEF1 (Lymphoid Enhancer Binding Factor 1). This transcription factor contains a high mobility group (HMG) DNA-binding domain, and is generally excessively expressed in malignant tumors. LEF1 promotes mesenchymal cell properties in EMT [59, 60] and was significantly associated with the overall survival of glioma patients. Reports indicate that the reduced expression of LEF1

inhibited cell migration, invasion, and EMT in glioblastoma cells [61]. In our study, the changes in the *LEF1* gene were confined to diffuse glioma and glioblastoma. Its mRNA expression levels were significantly higher in grades 3 and 4 as compared to grade 2, which was not backed up with our qRT-PCR results.

A type-3 intermediate filament protein, vimentin, encoded by *VIM,* is another well-known mesenchymal marker responsible for cytoskeletal interactions. It functions as an organizer of several other key proteins involved in cell attachment, migration and signaling [62]. Glioma types sustained different changes, –in glioblastoma the gene was mutated and in diffuse gliomas, it was predominantly amplified. Higher levels of mRNA expression were noted, and significant differences in the expression levels were recorded between grades 2 and 3, 2 and 4, and 3 and 4, where higher mRNA levels were associated with higher grades according to GlioVis, which was corroborated with qRT-PCR. Generally, the activation of EMT–TFs leads to the decreased expression of epithelial markers and increased expression of mesenchymal markers. They all bind to the E-box, the *cis*-regulatory element of the *CDH1* gene, and thus act as repressors of E-cadherin expression [63, 64]. Our study showed that genes for transcription factors from the protein families SNAIL, ZEB, and TWIST were mostly altered by mutations and amplifications in HGG. It is known that transcriptional repressor TWIST1, through binding to E-cadherin's promoter or by inducing SNAI1, promotes chromosomal instability, angiogenesis, invasion, metastasis, and resistance to chemotherapy [65, 66]. SNAI1 (SNAIL) and SNAI2 (SLUG) are zinc-finger transcription factors that maintain mesenchymal and an undifferentiated phenotype by controlling invasive characteristics [57, 59, 67, 68]. ZEB1 and ZEB2 are two closely related EMT transcriptional regulators of the Zinc Finger E-box Binding Homeobox family. The role of both ZEBs is to promote EMT, tumor progression, and metastasis through E-cadherin downregulation. It has also been documented that their overexpression has been found in several cancers and that they are responsible for therapy resistance [69-71]. It is known that ZEB1/2 are highly regulated in the early stage of hybrid EMT and their high level is maintained in mesenchymal cell populations [69]. ZEB2 has previously been confirmed to be associated with the malignant phenotype of glioma [72] and expression level of ZEB1 was significantly increased in glioma tissues compared to normal brain tissues being positively correlated with WHO glioma classification [73]. In this investigation, we have shown that *ZEB1* and *ZEB2* mutations were more common in high-grade gliomas and that qRT-PCR results showed higher transcript levels in HGG as compared to LGG and normal brain. However, GlioVis

reported on significant downregulation of both transcripts in grade 4 tumors as compared to 3, which was contrary toour qRT-PCR results. Furthermore, we have shown that *TWIST1* was altered predominately by amplifications in glioblastoma and diffuse glioma. Additionally, its transcript was significantly higher in higher glioma grades, which was confirmed by qRT-PCR validation. TWIST1 was related to shorter overall survival (p=0.018), and for age adjusted survival in *IDH1* wt and mutant glioblastomas TWIST1 was again indicated as almost significant (p = 0.079).

It was recently reported that the transcriptional repressors of the snail family, SNAI1 and SNAI2 play a role in the acquisition and increase of invasiveness in malignant gliomas [67, 68]. It has been shown that SNAI1 induces EMT, through the expression of EMT markers. SNAI2 expression was increased in glioblastomas compared to healthy brain tissue [74, 75]. SNAI1 and SNAI2 transcript levels rose in higher grades according to GlioVis. SNAI1 protein levels were also high in glioblastoma according to cBioPortal. qRT-PCR data were partially compatible with GlioVis for *SNAI1,* and *SNAI2,* for showing higher levels in LGG when compared to controls, but discordant for lower levels in HGG.

Potential explanations for evidenced discrepancies could be explained by post-transcriptional regulation, tumor heterogeneity, or technical limitations in sample processing. We also investigated post-transcriptional regulation, by analyzing methylation patterns to provide additional insights into the underlying disease mechanisms and patterns. mRNA expression levels were associated to levels of methylation for genes *CDH1, NOTCH1, TJP1/ZO-1, SNAI1, SNAI2*, and *VIM*.

Differential expression analysis stratified for *IDH1* mutations showed that *IDH* mutant samples had significantly lower *CDH2, LEF1* and *SNAI1* expression, while *ZEB1* significantly higher. Gene expression in different glioblastoma subtypes showed that *TJP1/ZO-1* gene was associated with classical subtype, while *ZEB2* with proneural one.

Our study showed that all genes representative of EMT are mutated or changed in certain ways in gliomas and that some show a marked involvement and are associated with a higher grade of glioma. Statistical analysis showed differences when looking at the overall changes in the pathohistological glioma types. Thus, astrocytomas harbored more changes in selected genes, *i.e.* all genes were affected. Furthermore, the accumulation of changes from diffuse gliomas to glioblastoma is visible in all examined genes, where changes in the *NOTCH1* and *SOX2* genes were most pronounced. Our findings could be connected to the concept of hybrid

EMT, a state in which tumor cells have both mesenchymal and epithelial features, which makes them especially flexible in adapting to the new tumor microenvironment [4, 5, 8]. Observed gene expression patterns (e.g., co-occurrence of epithelial and mesenchymal markers) support partial EMT in gliomas. Several recent studies give evidence on EMT plasticity of glioma cells. A paper reports on cancer stemness-associated genes in gliomas determined by their relative mRNA expression [76].

We have to mention another possible mechanism contributing to EMT plasticity, for instance RNA interference [77]. A study by [78] Qu et al. indicated that Hsa-miR-196a-5p overexpression was associated with clinical malignant biological behavior of glioma.

Immune cell infiltration is also vital for glioma microenvironment [79,80]. Important research was conducted on the proinflammatory-related molecules as promising immune biomarkers significantly associated with clinical indicators of malignant progression in glioma patients. Tumor-infiltrating immune cells are strongly associated with tumorigenesis and progression, for instance transcription factor CASZ1 [81, 82] was significantly upregulated in gliomas and was related to EMT-signaling. At present, there are many studies on the latest prognostic biomarkers and targets of glioma. [76 - 83]. The plasticity of hybrid EMT allows cancer cells to adapt to environmental stress during malignant progression. Our validation by qRT-PCR demonstrated that the levels of *CDH1, LEF1,* and *TJP1/ZO-1,* were lower in both LGG and HGG in comparison to normal controls. *CTNNB1*, *TWIST1, VIM, ZEB1*, and *ZEB2* had higher levels in HGG than LGG, while *SOX2*, *NOTCH1, SNAI1, SNAI2 and* CDH*2*, had higher levels in LGG than HGG.

It is also important to highlight that the enrichment analysis indicated pathways where the genes we investigated are interconnected. The pathways that emerged as significantly enriched were two epithelial to mesenchymal transition pathways and CCL18 signaling that led to several EMT pathways or migration and invasiveness.

Although our current study is primarily bioinformatics-based, experimental validation would certainly advance the causality of this research direction. In order to functionally validate key drivers, NOTCH1 and SOX2, prospective future studies based on strategies of knock-down experiments, invasion and migration assays need to be additionally conducted to confirm the causal role of these genes in EMT phenotypes. For that purpose glioblastoma cell lines (e.g., U87, LN229) should be used for knockdown experiments targeting NOTCH1 and SOX2 via siRNA transfection. Cells will be transfected with siNOTCH1 and siSOX2, alongside a non-

targeting siRNA control, using Lipofectamine or equivalent transfection reagents following the manufacturer's protocol. Following knockdown, EMT-associated phenotypes needs to be assesed, including proliferation, migration, and invasion. Migration and invasion will be evaluated using Transwell chamber assays, while proliferation will be assessed using MTT or BrdU incorporation assays. Additional research involving functional experiments is needed to establish causality between gene alterations and EMT phenotypes and confirm the knowledge that this work has brought.

CONCLUSION

This comprehensive study shows that genes associated with mesenchymal transition *CDH1*, *CTNNB1*, *TJP1*, *TWIST1*, *SOX2*, *ZEB1,* and *ZEB2* have higher frequencies of alterations in HGG versus LGG, indicating a shift toward more invasive phenotype. Of those genes, *CTNNB1*, *TWIST1, VIM, ZEB1*, and *ZEB2* had higher expression levels in HGG than LGG, while *SOX2*, *NOTCH1, SNAI1, SNAI2* and *CDH2*, had higher levels in LGG. In comparison to controls, low levels of transcripts of markers of epithelial phenotype *CDH1* and *TJP1* were recorded. Overall, *NOTCH1* and *SOX2*, key regulators of EMT, are most frequently altered both in HGG and LGG, indicating their universal role across different glioma tumors. These results provide valuable insights into the molecular differences between low- and high-grade gliomas, emphasizing the potential relevance of EMT-related genes in glioma biology and patient prognosis.

Conflicts of interests: Authors declare no conflicts of interest..

Funding: International bilateral research project Croatia-Slovenia MZOM
Slovenian Research and Innovation agency (International bilateral research project Slovenia – Croatia, P1-0390 and Z3-4510)
Croatian Science Foundation, "NeuroReact" project (IP2016-06-8636)
University of Zagreb support 10106-23-2393
University of Zagreb support 10106-24-1546
University of Zagreb support 10106-24-1372

Data availability: All data generated or analyzed during this study are included in this published article.

Submitted: 29 April 2025
Accepted: 05 July 2025
Published online: 17 July 2025

REFERENCES

[1] Chen T, You Y, Jiang H, Wang ZZ. Epithelial–mesenchymal transition (EMT): A biological process in the development, stem cell differentiation, and tumorigenesis. J Cell Physiol 2017;232:3261–3272. doi: 10.1002/jcp.25797. https://doi.org/10.1002/jcp.25797

[2] Brabletz S, Schuhwerk H, Brabletz T, Stemmler MP. Dynamic EMT: a multi-tool for tumor progression. EMBO J 2021;40(18):e108647. doi:10.15252/embj.2021108647. https://doi.org/10.15252/embj.2021108647

[3] Hanahan D, Weinberg RA. Hallmarks of cancer: The next generation. Cell 2011;144:646–674. doi: 10.1016/j.cell.2011.02.013. https://doi.org/10.1016/j.cell.2011.02.013

[4] Saitoh M. Involvement of partial EMT in cancer progression. J Biochem 2018;164:257–264. doi:10.1093/jb/mvy047. https://doi.org/10.1093/jb/mvy047

[5] Pastushenko I, Blanpain C. EMT transition states during tumor progression and metastasis. Trends Cell Biol 2019;29:212–226. doi: 10.1016/j.tcb.2018.12.001. https://doi.org/10.1016/j.tcb.2018.12.001

[6] Nieto MA. The ins and outs of the epithelial to mesenchymal transition in health and disease. Annu Rev Cell Dev Biol 2011;27:347–376. doi: 10.1146/annurev-cellbio-092910-154036. https://doi.org/10.1146/annurev-cellbio-092910-154036

[7] Loh CY, Chai JY, Tang TF, Wong WF, Sethi G, Shanmugam MK, et al. The E-cadherin and N-cadherin switch in epithelial-to-mesenchymal transition: Signaling, therapeutic implications, and challenges. Cells 2019;8:1118. doi: 10.3390/cells8101118. https://doi.org/10.3390/cells8101118

[8] Aiello NM, Kang Y. Context-dependent EMT programs in cancer metastasis. J Exp Med 2019;216(5):1016–1026. doi:10.1084/jem.20181827. https://doi.org/10.1084/jem.20181827

[9] Mrozik KM, Blaschuk OW, Cheong CM, Zannettino ACW, Vandyke K. N-cadherin in cancer metastasis, its emerging role in haematological malignancies and potential as a therapeutic target in cancer. BMC Cancer 2018;18(1):939. doi: 10.1186/s12885-018-4845-0. https://doi.org/10.1186/s12885-018-4845-0

[10] Xing Y, He M, Su Z, Yasinjan F, Liu J, Wang H, et al. Emerging trends and research foci of epithelial–mesenchymal transition in gliomas: a scientometric analysis and review.

Front Oncol 2022;12:1015236. doi:10.3389/fonc.2022.1015236. https://doi.org/10.3389/fonc.2022.1015236

[11] Chen R, Smith-Cohn ML, Cohen A, Colman H. Glioma subclassifications and their clinical significance. Neurotherapeutics 2017;14(2):284-297. doi: 10.1007/s13311-017-0519-x. https://doi.org/10.1007/s13311-017-0519-x

[12] Louis DN, Perry A, Wesseling P, Brat DJ, Cree IA, Figarella-Branger D, et al. The 2021 WHO classification of tumors of the central nervous system: a summary. Neuro Oncol 2021;23(8):1231-1251. doi: 10.1093/neuonc/noab106. https://doi.org/10.1093/neuonc/noab106

[13] Park YW, Vollmuth P, Foltyn-Dumitru M, Sahm F, Ahn SS, Chang JH, et al. The 2021 WHO classification for gliomas and implications on imaging diagnosis: part 1-key points of the fifth edition and summary of imaging findings on adult-type diffuse gliomas. J Magn Reson Imaging 2023;58:677–689. doi: 10.1002/jmri.28743. https://doi.org/10.1002/jmri.28743

[14] Cerami E, Gao J, Dogrusoz U, Gross BE, Sumer SO, Aksoy BA, et al. The cBio cancer genomics portal: an open platform for exploring multidimensional cancer genomics data. Cancer Discov 2012;2(5):401-04. doi: 10.1158/2159-8290.CD-12-0095. https://doi.org/10.1158/2159-8290.CD-12-0095

[15] Gao J, Aksoy BA, Dogrusoz U, Dresdner G, Gross B, Sumer SO, et al. Integrative analysis of complex cancer genomics and clinical profiles using the cBioPortal. Sci Signal 2013;6(269):pl1. doi: 10.1126/scisignal.2004088. https://doi.org/10.1126/scisignal.2004088

[16] Barthel FP, Johnson KC, Varn FS, Moskalik AD, Tanner G, Kocakavuk E, et al. GLASS Consortium. Longitudinal molecular trajectories of diffuse glioma in adults. Nature. 2019 Dec;576(7785):112-120. doi: 10.1038/s41586-019-1775-1. https://doi.org/10.1038/s41586-019-1775-1

[17] Jonsson P, Lin AL, Young RJ, DiStefano NM, Hyman DM, Li BT, et al. Genomic Correlates of Disease Progression and Treatment Response in Prospectively Characterized Gliomas. Clin Cancer Res. 2019 Sep 15;25(18):5537-5547. doi: 10.1158/1078-0432.CCR-19-0032. https://doi.org/10.1158/1078-0432.CCR-19-0032

[18] Johnson BE, Mazor T, Hong C, Barnes M, Aihara K, McLean CY, et al. Mutational analysis reveals the origin and therapy-driven evolution of recurrent glioma. Science. 2014

Jan 10;343(6167):189-193. doi: 10.1126/science.1239947. https://doi.org/10.1126/science.1239947

[19] Ceccarelli M, Barthel FP, Malta TM, Sabedot TS, Salama SR, Murray BA, et al. TCGA Research Network; Noushmehr H, Iavarone A, Verhaak RG. Molecular Profiling Reveals Biologically Discrete Subsets and Pathways of Progression in Diffuse Glioma. Cell. 2016 Jan 28;164(3):550-63. doi: 10.1016/j.cell.2015.12.028. https://doi.org/10.1016/j.cell.2015.12.028

[20] Vaubel RA, Tian S, Remonde D, Schroeder MA, Mladek AC, Kitange GJ, et al. Genomic and Phenotypic Characterization of a Broad Panel of Patient-Derived Xenografts Reflects the Diversity of Glioblastoma. Clin Cancer Res. 2020 Mar 1;26(5):1094-1104. doi: 10.1158/1078-0432.CCR-19-0909. https://doi.org/10.1158/1078-0432.CCR-19-0909

[21] Wang LB, Karpova A, Gritsenko MA, Kyle JE, Cao S, Li Y, et al. Clinical Proteomic Tumor Analysis Consortium. Proteogenomic and metabolomic characterization of human glioblastoma. Cancer Cell. 2021 Apr 12;39(4):509-528.e20. doi: 10.1016/j.ccell.2021.01.006. https://doi.org/10.1016/j.ccell.2021.01.006

[22] Zhao J, Chen AX, Gartrell RD, Silverman AM, Aparicio L, Chu T, et al. Immune and genomic correlates of response to anti-PD-1 immunotherapy in glioblastoma. Nat Med. 2019 Mar;25(3):462-469. doi: 10.1038/s41591-019-0349-y. https://doi.org/10.1038/s41591-019-0349-y

[23] The cBioPortal for Cancer Genomics [Internet] [accessed March 2025.]. Available from: https://www.cbioportal.org/results/comparison?cancer_study_list=difg_glass_2019%2Cglioma_mskcc_2019%2Clgggbm_tcga_pub%2Cgbm_mayo_pdx_sarkaria_2019%2Cgbm_cptac_2021%2Cgbm_columbia_2019%2Cgbm_tcga%2Clgg_ucsf_2014&Z_SCORE_THRESHOLD=2.0&RPPA_SCORE_THRESHOLD=2.0&profileFilter=mutations%2Cstructural_variants%2Cgistic%2Ccna&case_set_id=all&gene_list=CDH1%250ACDH2%250ACTNNB1%250ALEF1%250ANOTCH1%250ASNAI1%250ASNAI2%250ASOX2%250ATJP1%250ATWIST1%250AVIM%250AZEB1%250AZEB2&geneset_list=%20&tab_index=tab_visualize&Action=Submit&comparison_subtab=survival&comparison_selectedGroups=%5B%22CDH1%22%2C%22CDH2%22%2C%22CTNNB1%22%2C%22LEF1%22%2C%22NOTCH1%22%2C%22SNAI1%22%5D. or https://bit.ly/46n1Zai

[24] Bowman RL, Wang Q, Carro A, Verhaak RG, Squatrito M. GlioVis data portal for visualization and analysis of brain tumor expression datasets. Neuro Oncol 2017;19(1):139–41. doi:10.1093/neuonc/now247. https://doi.org/10.1093/neuonc/now247

[25] Li B, Dewey CN. RSEM: Accurate transcript quantification from RNA-Seq data with or without a reference genome. BMC Bioinform 2011;12:323. doi: 10.1186/1471-2105-12-323. https://doi.org/10.1186/1471-2105-12-323

[26] Hoadley KA, Yau C, Hinoue T, Wolf DM, Lazar A, Drill E, et al. Cell-of-origin patterns dominate the molecular classification of 10,000 tumors from 33 types of cancer. Cell 2018;173:291–304. doi: 10.1016/j.cell.2018.03.022. https://doi.org/10.1016/j.cell.2018.03.022

[27] Jovčevska I, Zupanec N, Urlep Ž, Vranič A, Matos B, Stokin CL, et al. Differentially expressed proteins in glioblastoma multiforme identified with a nanobody-based anti-proteome approach and confirmed by OncoFinder as possible tumor-class predictive biomarker candidates. Oncotarget 2017;8(27):44141–158. doi: 10.18632/oncotarget.17390. https://doi.org/10.18632/oncotarget.17390

[28] Bustin SA, Benes V, Garson JA, Hellemans J, Huggett J, Kubista M, Mueller R, Nolan T, Pfaffl MW, Shipley GL, Vandesompele J, Wittwer CT. The MIQE guidelines: minimum information for publication of quantitative real-time PCR experiments. Clin Chem. 2009 Apr;55(4):611-22. doi: 10.1373/clinchem.2008.112797. https://doi.org/10.1373/clinchem.2008.112797

[29] Livak, K. J., & Schmittgen, T. D. (2001). Analysis of relative gene expression data using real-time quantitative PCR and the 2(-Delta Delta C(T)) Method. Methods (San Diego, Calif.), 25(4), 402–408. https://doi.org/10.1006/meth.2001.1262

[30] Szklarczyk D, Nastou K, Koutrouli M, Kirsch R, Mehryary F, Hachilif R, Hu D, Peluso ME, Huang Q, Fang T, Doncheva NT, Pyysalo S, Bork P, Jensen LJ, von Mering C. The STRING database in 2025: protein networks with directionality of regulation. Nucleic Acids Res. 2025 Jan 6;53(D1):D730-D737. doi: 10.1093/nar/gkae1113 https://doi.org/10.1093/nar/gkae1113

[31] Szklarczyk D, Kirsch R, Koutrouli M, Nastou K, Mehryary F, Hachilif R, et al. The STRING database in 2023: protein-protein association networks and functional enrichment analyses for any sequenced genome of interest. Nucleic Acids Res 2023;51(D1):D638–D646. doi:10.1093/nar/gkac1000. https://doi.org/10.1093/nar/gkac1000

[32] Sinha D, Saha P, Samanta A, Bishayee A. Emerging concepts of hybrid epithelial-to-mesenchymal transition in cancer progression. Biomolecules 2020;10(11):1561. doi:10.3390/biom10111561. https://doi.org/10.3390/biom10111561

[33] Wu H, Wei M, Li Y, Ma Q, Zhang H. Research progress on the regulation mechanism of key signal pathways affecting the prognosis of glioma. Front Mol Neurosci 2022;15:910543. doi:10.3389/fnmol.2022.910543. https://doi.org/10.3389/fnmol.2022.910543

[34] Haerinck J, Berx G. Partial EMT takes the lead in cancer metastasis. Dev Cell 2021;56(23):3174-76. doi: 10.1016/j.devcel.2021.11.012. https://doi.org/10.1016/j.devcel.2021.11.012

[35] Uhlmann K, Rohde K, Zeller C, Szymas J, Vogel S, Marczinek K, et al. Distinct methylation profiles of glioma subtypes. Int J Cancer 2003;106(1):52–9. doi:10.1002/ijc.11175. https://doi.org/10.1002/ijc.11175

[36] Pećina-Šlaus N. Tumor suppressor gene E-cadherin and its role in normal and malignant cells. Cancer Cell Int 2003;3(1):17. doi: 10.1186/1475-2867-3-17. https://doi.org/10.1186/1475-2867-3-17

[37] Venhuizen JH, Jacobs FJC, Span PN, Zegers MM. P120 and E-cadherin: double-edged swords in tumor metastasis. Semin Cancer Biol 2020;60:107–20. doi:10.1016/j.semcancer.2019.07.020. https://doi.org/10.1016/j.semcancer.2019.07.020

[38] Schwechheimer K, Zhou L, Birchmeier WE. Cadherin in human brain tumours: loss of immunoreactivity in malignant meningiomas. Virchows Arch 1998;432:163–7. doi:10.1007/s004280050151. https://doi.org/10.1007/s004280050151

[39] Runkle EA, Mu D. Tight junction proteins: from barrier to tumorigenesis. Cancer Lett. 2013;337(1):41-8. doi:10.1016/j.canlet.2013.05.038. https://doi.org/10.1016/j.canlet.2013.05.038

[40] Hazan RB, Qiao R, Keren R, Badano I, Suyama K. Cadherin switch in tumor progression. Ann N Y Acad Sci 2004;1014:155–63. doi: 10.1196/annals.1294.016. https://doi.org/10.1196/annals.1294.016

[41] Dongre A, Weinberg RA. New insights into the mechanisms of epithelial–mesenchymal transition and implications for cancer. Nat Rev Mol Cell Biol 2019;20:69–84. doi: 10.1038/s41580-018-0080-4. https://doi.org/10.1038/s41580-018-0080-4

[42] Chen Q, Cai J, Jiang C. CDH2 expression is of prognostic significance in glioma and predicts the efficacy of temozolomide therapy in patients with glioblastoma. Oncol Lett 2018;15(5):7415-22. doi: 10.3892/ol.2018.8227. https://doi.org/10.3892/ol.2018.8227

[43] Xiong Y, Liu L, Zhu S, Zhang B, Qin Y, Yao R, et al. Precursor N-cadherin mediates glial cell line-derived neurotrophic factor-promoted human malignant glioma. Oncotarget 2017;8(15):24902–914. doi:10.18632/oncotarget.15302. https://doi.org/10.18632/oncotarget.15302

[44] Wang Z, Li Y, Banerjee S, Sarkar FH. Emerging role of Notch in stem cells and cancer. Cancer Lett 2009;279:8–12. doi:10.1016/j.canlet.2008.09.030. https://doi.org/10.1016/j.canlet.2008.09.030

[45] Shi Q, Xue C, Zeng Y, Yuan X, Chu Q, Jiang S, et al. Notch signaling pathway in cancer: from mechanistic insights to targeted therapies. Signal Transduct Target Ther 2024;9(1):128. doi:10.1038/s41392-024-01828-x. https://doi.org/10.1038/s41392-024-01828-x

[46] Timmerman LA, Grego-Bessa J, Raya A, Bertrán E, Pérez-Pomares JM, Díez J, et al. Notch promotes epithelial-mesenchymal transition during cardiac development and oncogenic transformation. Genes Dev 2004;18:99–115. doi:10.1101/gad.276304. https://doi.org/10.1101/gad.276304

[47] Zavadil J, Cermak L, Soto-Nieves N, Bottinger EP. Integration of TGF-beta/Smad and Jagged1/Notch signalling in epithelial-to-mesenchymal transition. EMBO J 2004;23:1155–65. doi:10.1038/sj.emboj.7600069. https://doi.org/10.1038/sj.emboj.7600069

[48] Zhang Q, Wang J, Zhang J, Wang Y, Wang Y, Liu F. Cancer-associated fibroblasts-induced remodeling of tumor immune microenvironment via Jagged1 in glioma. Cell Signal 2024;115:111016. doi:10.1016/j.cellsig.2023.111016. https://doi.org/10.1016/j.cellsig.2023.111016

[49] Yi L, Zhou X, Li T, Liu P, Hai L, Tong L, et al. Notch1 signaling pathway promotes invasion, self-renewal and growth of glioma initiating cells via modulating chemokine system CXCL12/CXCR4. J Exp Clin Cancer Res 2019;38(1):339. doi:10.1186/s13046-019-1319-4. https://doi.org/10.1186/s13046-019-1319-4

[50] Zhao G, Deng Z, Li X, Wang H, Chen G, Feng M, Zhou Y. Targeting EZH2 regulates the biological characteristics of glioma stem cells via the Notch1 pathway. Exp Brain Res 2023;241(10):2409–18. doi:10.1007/s00221-023-06693-8. https://doi.org/10.1007/s00221-023-06693-8

[51] Xu YR, Yang WX. SOX-mediated molecular crosstalk during the progression of tumorigenesis. Semin Cell Dev Biol 2017;63:23–34. doi:10.1016/j.semcdb.2016.07.028. https://doi.org/10.1016/j.semcdb.2016.07.028

[52] Kim O, Sergi Z, Yu G, Yamamoto K, Quezado M, Abdullaev Z, et al. A patient-derived cell model for malignant transformation in IDH-mutant glioma. Acta Neuropathol Commun 2024;12(1):148. doi: 10.1186/s40478-024-01860-6. https://doi.org/10.1186/s40478-024-01860-6

[53] Guetta-Terrier C, Karambizi D, Akosman B, Zepecki JP, Chen JS, Kamle S, et al. Chi3l1 is a modulator of glioma stem cell states and a therapeutic target in glioblastoma. Cancer Res 2023;83(12):1984-99. doi: 10.1158/0008-5472.CAN-21-3629. https://doi.org/10.1158/0008-5472.CAN-21-3629

[54] Song H, Zhang Y, Liu N, Zhao S, Kong Y, Yuan L. miR-92a-3p exerts various effects in glioma and glioma stem-like cells specifically targeting CDH1/β-catenin and Notch-1/Akt signaling pathways. Int J Mol Sci 2016;17(11):1799. doi:10.3390/ijms17111799. https://doi.org/10.3390/ijms17111799

[55] Pećina-Šlaus N, Kafka A, Tomas D, Marković L, Okštajner PK, Sukser V, et al. Wnt signaling transcription factors TCF-1 and LEF-1 are upregulated in malignant astrocytic brain tumors. Histol Histopathol 2014;29(12):1557-64. doi: 10.14670/HH-29.1557. https://doi.org/10.14670/HH-29.1557

[56] Du L, Lee J-H, Jiang H, Wang C, Wang S, Zheng Z, et al. β-Catenin induces transcriptional expression of PD-L1 to promote glioblastoma immune evasion. J Exp Med 2020;217(11):e20191115. doi: 10.1084/jem.20191115. https://doi.org/10.1084/jem.20191115

[57] Yang J, Antin P, Berx G, Blanpain C, Brabletz T, Bronner M, et al. Guidelines and definitions for research on epithelial–mesenchymal transition. Nat Rev Mol Cell Biol 2022;21(6):341–52. doi:10.1038/s41580-020-0237-9. https://doi.org/10.1038/s41580-020-0237-9

[58] Yu X, Xiao F, Wei Y, Miao L, Zhang W, Zhang X, et al. Elevated β-catenin and C-myc promote malignancy, relapse, and indicate poor prognosis in patients with relapsed glioma. J Cancer Res Ther 2022;18(2):553–9. doi:10.4103/jcrt.jcrt_246_22. https://doi.org/10.4103/jcrt.jcrt_246_22

[59] Zirkel A, Lederer M, Stohr N, Pazaitis N, Huttelmaier S. IGF2BP1 promotes mesenchymal cell properties and migration of tumor-derived cells by enhancing the expression of LEF1 and SNAI2 (SLUG). Nucleic Acids Res 2013;41:6618–36. doi:10.1093/nar/gkt410. https://doi.org/10.1093/nar/gkt410

[60] Zhou X, Li X, Wang R, Hua D, Sun D, Yu L, et al. Recruitment of LEF1 by Pontin chromatin modifier amplifies TGFBR2 transcription and activates TGFβ/SMAD signalling during gliomagenesis. Cell Death Dis 2022;13(9):818. doi:10.1038/s41419-022-05265-y. https://doi.org/10.1038/s41419-022-05265-y

[61] Min R-Q, Ma Q. MicroRNA-381 inhibits metastasis and epithelial-mesenchymal transition of glioblastoma cells through targeting LEF1. Eur Rev Med Pharmacol Sci 2020;24(12):6825-33. doi: 10.26355/eurrev_202006_21672. https://doi.org/10.26355/eurrev_202006_21672

[62] Zottel A, Novak M, Šamec N, Majc B, Colja S, Katrašnik M, et al. Anti-Vimentin nanobody decreases glioblastoma cell invasion in vitro and in vivo. Cancers (Basel) 2023;15(3):573. doi:10.3390/cancers15030573. https://doi.org/10.3390/cancers15030573

[63] Das V, Bhattacharya S, Chikkaputtaiah C, Hazra S, Pal M. The basics of epithelial-mesenchymal transition (EMT): A study from a structure, dynamics, and functional perspective. J Cell Physiol 2019;234(9):14535-55. doi: 10.1002/jcp.28160. https://doi.org/10.1002/jcp.28160

[64] Saitoh M. Transcriptional regulation of EMT transcription factors in cancer. Semin Cancer Biol 2023;97:21-9. doi:10.1016/j.semcancer.2023.10.001. https://doi.org/10.1016/j.semcancer.2023.10.001

[65] Mikheeva SA, Mikheev AM, Petit A, Beyer R, Oxford RG, Khorasani L, et al. TWIST1 promotes invasion through mesenchymal change in human glioblastoma. Mol Cancer 2010;9:194. doi: 10.1186/1476-4598-9-194. https://doi.org/10.1186/1476-4598-9-194

[66] Mikheev AM, Mikheeva SA, Severs LJ, Funk CC, Huang L, McFaline-Figueroa JL, et al. Targeting TWIST1 through loss of function inhibits tumorigenicity of human glioblastoma. Mol Oncol 2018;12(7):1188-202. doi: 10.1002/1878-0261.12320. https://doi.org/10.1002/1878-0261.12320

[67] Han S-P, Kim J-H, Han M-E, Sim H-E, Kim K-S, Yoon S, et al. SNAI1 is involved in the proliferation and migration of glioblastoma cells. Cell Mol Neurobiol 2011;31(3):489-96. doi: 10.1007/s10571-010-9643-4. https://doi.org/10.1007/s10571-010-9643-4

[68] Kaji T, Arito M, Tsutiya A, Sase T, Onodera H, Sato T, et al. Layilin enhances the invasive ability of malignant glioma cells via SNAI1 signaling. Brain Res 2019;1719:140-7. doi: 10.1016/j.brainres.2019.05.034. https://doi.org/10.1016/j.brainres.2019.05.034

[69] Korpal M, Lee ES, Hu G, Kang Y. The miR-200 family inhibits epithelial-mesenchymal transition and cancer cell migration by direct targeting of E-cadherin transcriptional repressors ZEB1 and ZEB2. J Biol Chem 2008;283(22):14910-14. doi: 10.1074/jbc.C800074200. https://doi.org/10.1074/jbc.C800074200

[70] Baqai N, Amin R, Fatima T, Ahmed Z, Faiz N. Expression profiling of EMT transcriptional regulators ZEB1 and ZEB2 in different histopathological grades of oral squamous cell carcinoma patients. Curr Genomics 2024;25(2):140–51. doi: 10.2174/0113892029284920240212091903 https://doi.org/10.2174/0113892029284920240212091903

[71] Sun Y, Guo G, Zhang Y, Chen X, Lu Y, Hong R, et al. IKBKE promotes the ZEB2-mediated EMT process by phosphorylating HMGA1a in glioblastoma. Cell Signal 2024;116:111062. doi:10.1016/j.cellsig.2024.111062. https://doi.org/10.1016/j.cellsig.2024.111062

[72] Zeng Y, Que T, Lin J, Zhan Z, Xu A, Wu Z, et al. Oncogenic ZEB2/miR-637/HMGA1 signaling axis targeting vimentin promotes the malignant -mesenchymal transition of glioma cells promotes tissue factor expression via the miR200a/ZEB1 axis. Brain Res 2022;1778:147782. doi:10.1016/j.brainres.2022.147782. https://doi.org/10.1016/j.brainres.2022.147782

[73] Sun Y, Jiang Y, Wang Y, Yu P, Su X, Song Y, et al. The epithelial-mesenchymal transition of glioma cells promotes tissue factor expression via the miR200a/ZEB1 axis. Brain Res 2022;1778:147782. doi:10.1016/j.brainres.2022.147782. https://doi.org/10.1016/j.brainres.2022.147782

[74] Yang HW, Menon LG, Black PM, Carroll RS, Johnson MD. SNAI2/Slug promotes growth and invasion in human gliomas. BMC Cancer. 2010;10:301. doi:10.1186/1471-2407-10-301. https://doi.org/10.1186/1471-2407-10-301

[75] Kwon R-Y, Han M-E, Kim Y-J, Kim Y-H, Kim J-Y, Liu L, et al. Roles of zinc-fingers and homeoboxes 1 during the proliferation, migration, and invasion of glioblastoma cells.

Tumour Biol 2017;39(3):1010428317694575. doi: 10.1177/1010428317694575. https://doi.org/10.1177/1010428317694575

[76] Qu S, Huang J, Liu J, Wang H. Prognostic significance of cancer stemness-associated genes in patients with gliomas. Clinical and translational medicine 2020;10(5) e186. doi: 10.1002/ctm2.186. https://doi.org/10.1002/ctm2.186

[77] Hu Z, Rong Y, Li S, Qu S, Huang S. Upregulated Histone Deacetylase 6 Associates with Malignant Progression of Melanoma and Predicts the Prognosis of Patients. Cancer management and research 2020;12;12993-13001 doi: 10.2147/CMAR.S284199. https://doi.org/10.2147/CMAR.S284199

[78] Qu S, Qiu O, Huang J, Liu J, Wang H. Upregulation of hsa-miR-196a-5p is associated with MIR196A2 methylation and affects the malignant biological behaviors of glioma. Genomics 2021;113(3):1001-1010 doi: 10.1016/j.ygeno.2021.02.012, https://doi.org/10.1016/j.ygeno.2021.02.012

[79] Pećina-Šlaus N, Hrašćan R. Glioma Stem Cells-Features for New Therapy Design. Cancers (Basel). 2024 Apr 19;16(8):1557. doi: 10.3390/cancers16081557. https://doi.org/10.3390/cancers16081557

[80] Huang C, Qiu O, Mao C, Hu Z, Qu S. An integrated analysis of C5AR2 related to malignant properties and immune infiltration of gliomas. Cancer innovation 2022;1(3);240-251 doi: 10.1002/cai2.29. https://doi.org/10.1002/cai2.29

[81] Mao C, Huang C, Hu Z, Qu S. Transcription factor CASZ1 increases an oncogenic transcriptional process in tumorigenesis and progression of glioma cells. MedComm 2022;3(4) e182 doi: 10.1002/mco2.182. https://doi.org/10.1002/mco2.182

[82] Qu S, Huang C, Zhu T, Wang K, Zhang H, Wang L, Xu R, Zheng H, Yuan X, Liu G, Zhu R, Qu J, Yi G, Qi S. OLFML3, as a potential predictor of prognosis and therapeutic target for glioma, is closely related to immune cell infiltration. VIEW 2023;4;20220052 doi: doi/10.1002/VIW.20220052. https://doi.org/10.1002/VIW.20220052

[83] Qu S, Huang C, Hu Z. The PODNL1/AKT/$\boldsymbol{\beta}$-catenin signaling axis mediates glioma progression and sensitivity to temozolomide. Fundamental Research 2023 doi: 10.1016/j.fmre.2023.03.005. https://doi.org/10.1016/j.fmre.2023.03.005

TABLES AND FIGURES WITH LEGENDS

Table 1. Summary results of the analysis of all genes

	Glioma type					
	Anaplastic Oligodendro glioma (grade 3)	Oligodendro-glioma (grade 2)	Anaplastic Astrocytoma (grade 3)	Glioblastoma (grade 4)	Oligoastrocyto-ma (grade 2)	Diffuse glioma (grade 2)
Change						
Mutations	29.03%	16.79%	7.58%	5.91%	6.25%	4.91%
Amplifications	1.61%	2.92%	4.04%	4.00%	6.25%	4.91%
Deep deletions				0.54%		0.98%
Multiple alterations				0.12%		0.23%
Total		19.71%	11.62%	10.5%	12.5%	11,03%

Table 2. Concordance and discordance of expression data.

	CDH1	*CDH2*	*TJP1/ ZO-1*	*CTNNB1*	*LEF1*	*VIM*	*NOTCH1*	*SNAI1*	*SNAI2*	*TWIST1*	*SOX2*	*ZEB1*	*ZEB2*
cBioPortal and GlioVis	dis	con	con	con	con	con	uc	con	con	con	uc	uc	dis
GlioVis and qRT-PCR	con	con/ dis	con	con	dis	con	con	con/ dis	con/ dis	con	con	dis	dis
cBioPortal and qRT-PCR	dis	dis	con	con	dis	con	con	dis	dis	con	con	uc	con

con = concordance, dis = discordance, uc = unconclusive

Table 3. Results for survival, glioblastoma (GBM) subtype and expression (*in silico* and qRT-PCR) are presented for each gene. With stronger color are noted the strongest results, with weaker color results that are showing the trends. CLAS= classical subtype; PN= proneural subtype.

Gene	Survival (*IDH1*wt)	Survival (*IDH1* mut)	Subtype	Expression in GBM *IDH1* wt compared to Grade 2 and Grade 3 (*in silico*)	Expression in GBM *IDH1* wt compared to control (qPCR)
CDH1	-	-	-	-	-
CDH2	-	-	-	↑	-
TJP1/ZO-1	-	-	CLAS	↓	-
CTNNB1	(+; p=0.063)	-	-	↑	-
LEF1	-	-	-	↑	↓
NOTCH1	-	-	-	↓	↓
SNAI1	-	-	-	↑	-
SNAI2	-	-	-	↑	
SOX2	-	-	-	↓	↓
TWIST1	(+; p=0.079)	(+; p=0.074)	-	↑	-
VIM	-	-	-	↑	-
ZEB1	-	-	-	↓	-
ZEB2	-	-	PN	↓	-

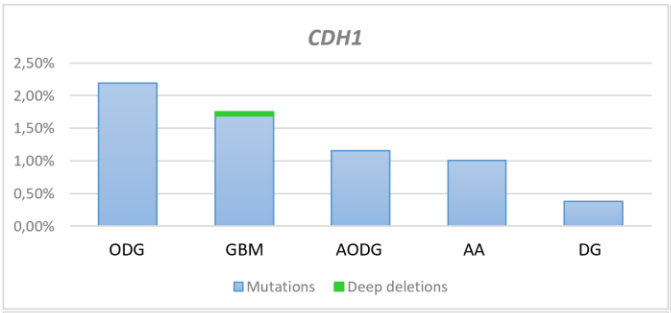
CDH1
2,50%
2,00%
1,50%
1,00%
0,50%
0,00%
ODG
GBM
AODG
AA
DG
Mutations
Deep deletions

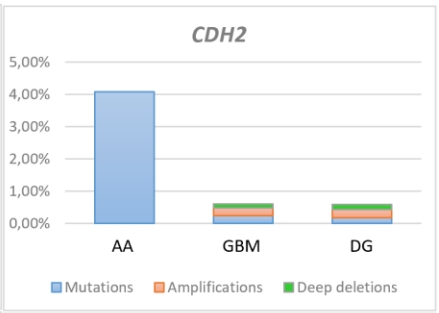
CDH2
5,00%
4,00%
3,00%
2,00%
1,00%
0,00%
AA
GBM
DG
Mutations
Amplifications
Deep deletions

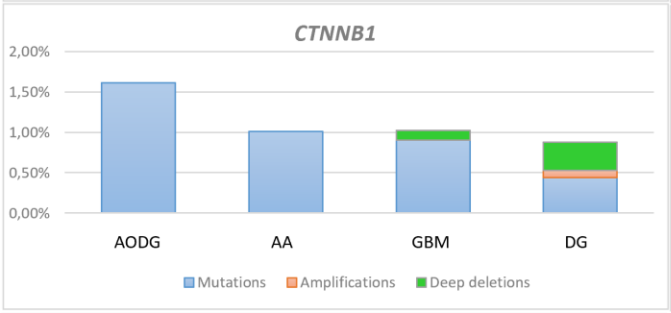
CTNNB1
2,00%
1,50%
1,00%
0,50%
0,00%
AODG
AA
GBM
DG
Mutations
Amplifications
Deep deletions

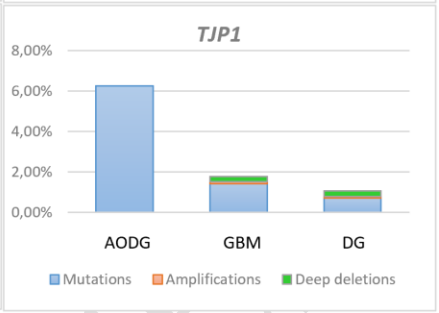
TJP1
8,00%
6,00%
4,00%
2,00%
0,00%
AODG
GBM
DG
Mutations
Amplifications
Deep deletions

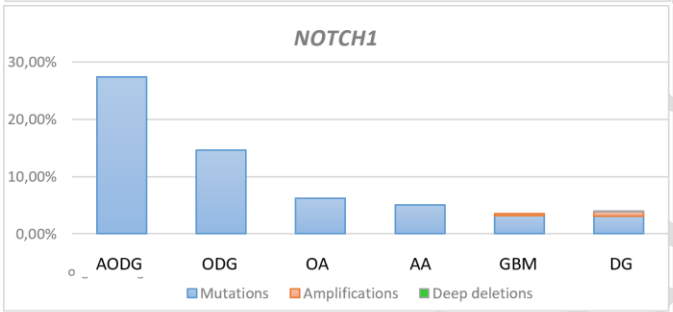
NOTCH1
30,00%
20,00%
10,00%
0,00%
AODG
ODG
OA
AA
GBM
DG
Mutations
Amplifications
Deep deletions

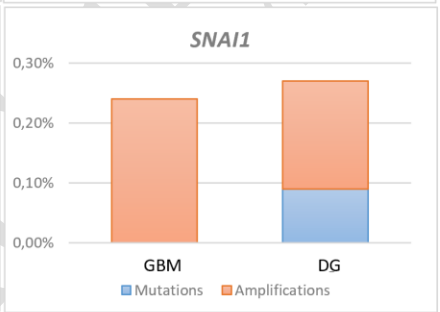
SNAI1
0,30%
0,20%
0,10%
0,00%
GBM
DG
Mutations
Amplifications

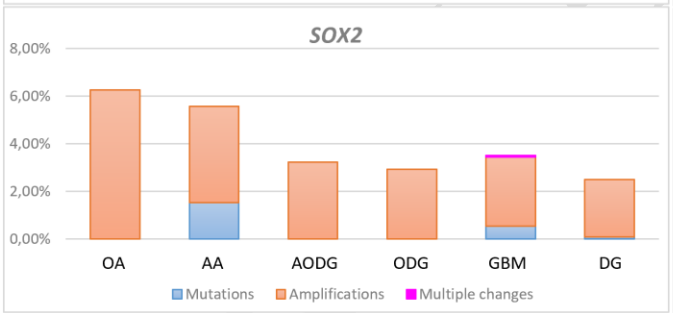
SOX2
8,00%
6,00%
4,00%
2,00%
0,00%
OA
AA
AODG
ODG
GBM
DG
Mutations
Amplifications
Multiple changes

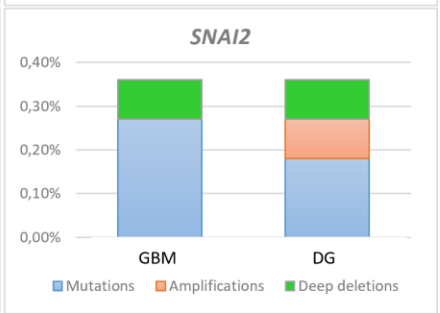
SNAI2
0,40%
0,30%
0,20%
0,10%
0,00%
GBM
DG
Mutations
Amplifications
Deep deletions

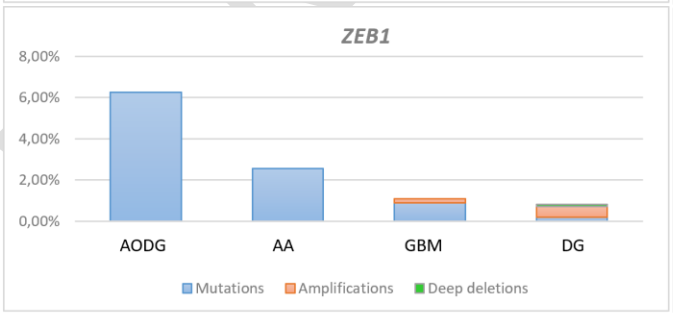
ZEB1
8,00%
6,00%
4,00%
2,00%
0,00%
AODG
AA
GBM
DG
Mutations
Amplifications
Deep deletions

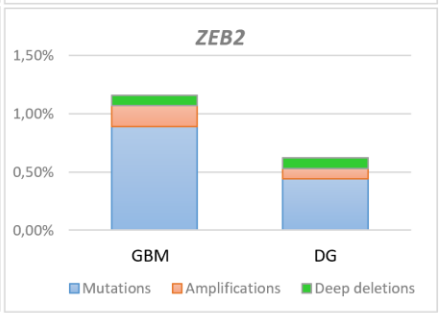
ZEB2
1,50%
1,00%
0,50%
0,00%
GBM
DG
Mutations
Amplifications
Deep deletions

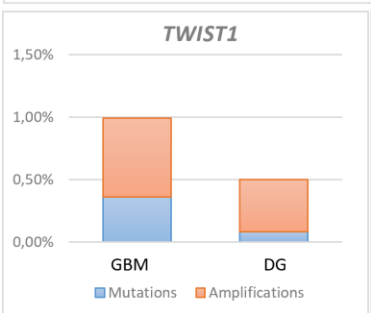
TWIST1
1,50%
1,00%
0,50%
0,00%
GBM
DG
Mutations
Amplifications

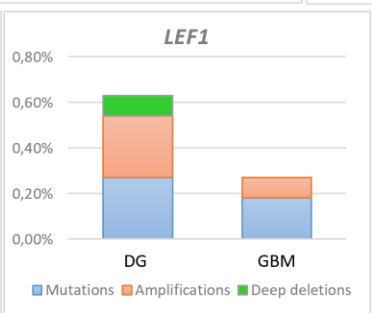
LEF1
0,80%
0,60%
0,40%
0,20%
0,00%
DG
GBM
Mutations
Amplifications
Deep deletions

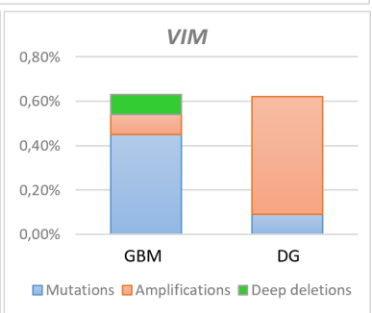
VIM
0,80%
0,60%
0,40%
0,20%
0,00%
GBM
DG
Mutations
Amplifications
Deep deletions

Figure 1. Results of gene analyses; *CDH1; CDH2; TJP1/ZO-1; CTNNB1; LEF1; VIM; NOTCH1; SNAI1; SNAI2; TWIST1; SOX2; ZEB1; ZEB2*. DG diffuse glioma; ODG oligodendroglioma; OA oligoastrocytoma; AODG anaplastic oligodendroglioma; AA anaplastic astrocytoma; GBM glioblastoma. Y-axis denotes the frequency of observed changes and X-axis glioma type.

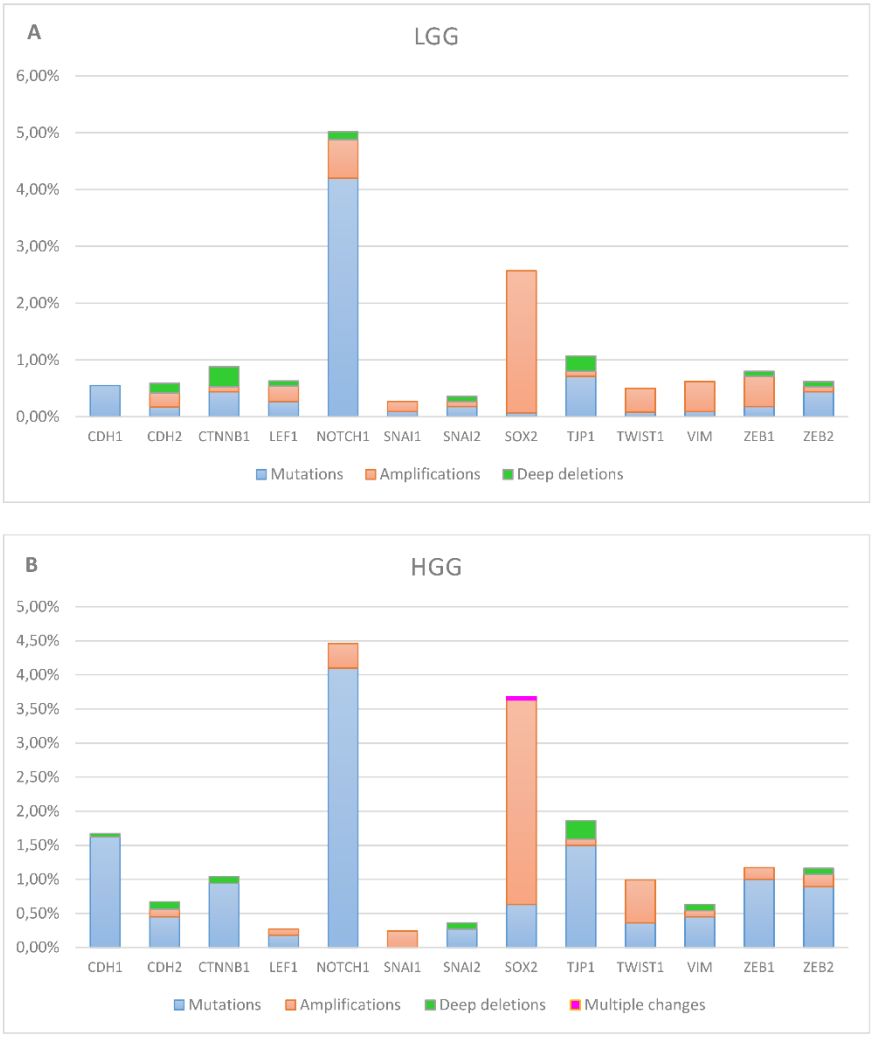

Figure 2. The overall presentation of changes in LGG (A) and HGG (B). Y-axis denotes the frequency of observed changes and X-axis genes. Type of changes is color coded in the legend.

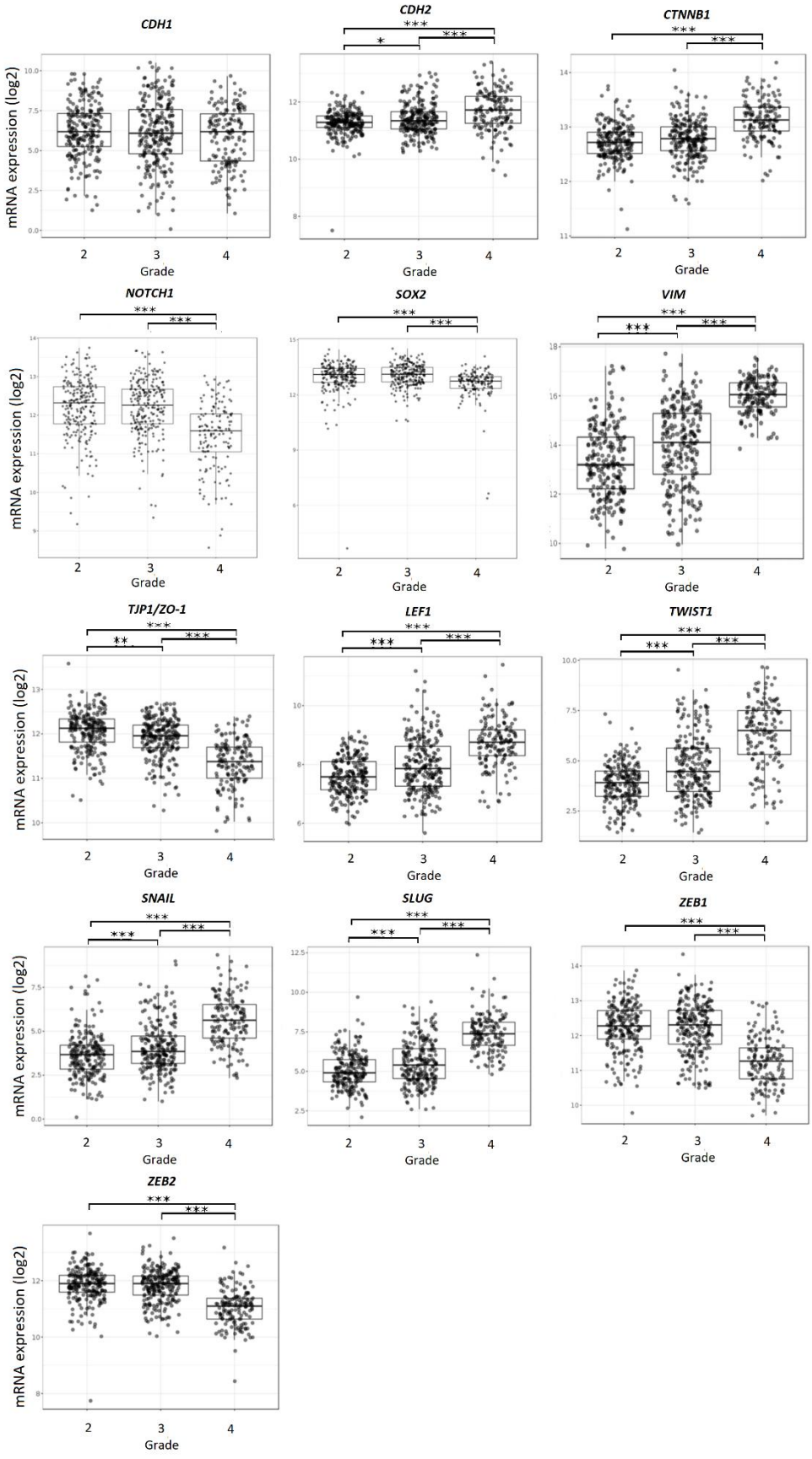
CDH1
CDH2
CTNNB1
NOTCH1
SOX2
VIM
TJP1/ZO-1
LEF1
TWIST1
SNAIL
SLUG
ZEB1
ZEB2
mRNA expression (log2)
Grade
2
3
4
***
**
*

Figure 3. Gene expression in glioma obtained from GlioVis, TCGA_GBMLGG dataset. Glioma grades 4, 3, and 2 were included in the study. Results are presented as mean +/- SD. * $p<0.05$, ** $p<0.01$, *** $p<0.001$, *** $p<0.0001$ (one-way ANOVA with Tukey's post hoc test).

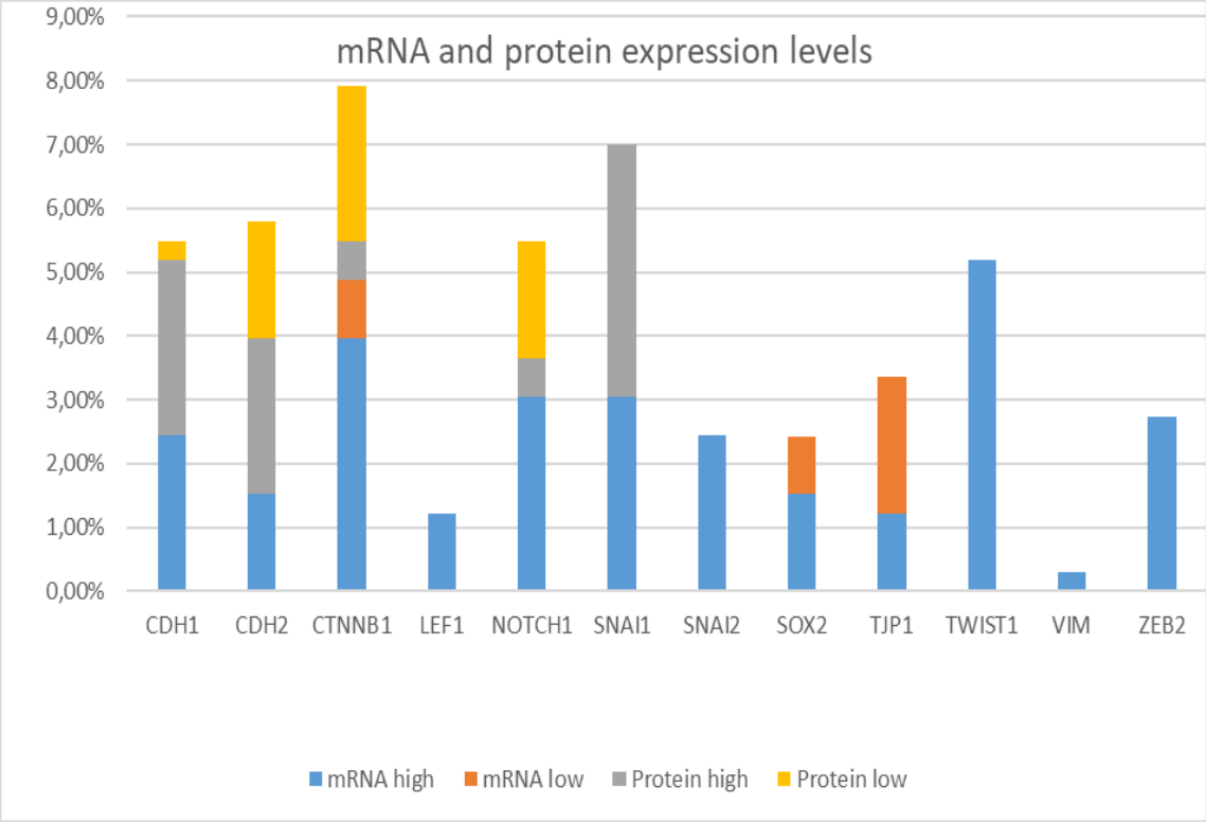

Figure 4. mRNA and protein expression levels. Samples from The Glioblastoma Multiforme study (TCGA, Firehose Legacy) obtained by next-generation sequencing from RNASeq V2 RSEM, downloaded from cBioPortal.

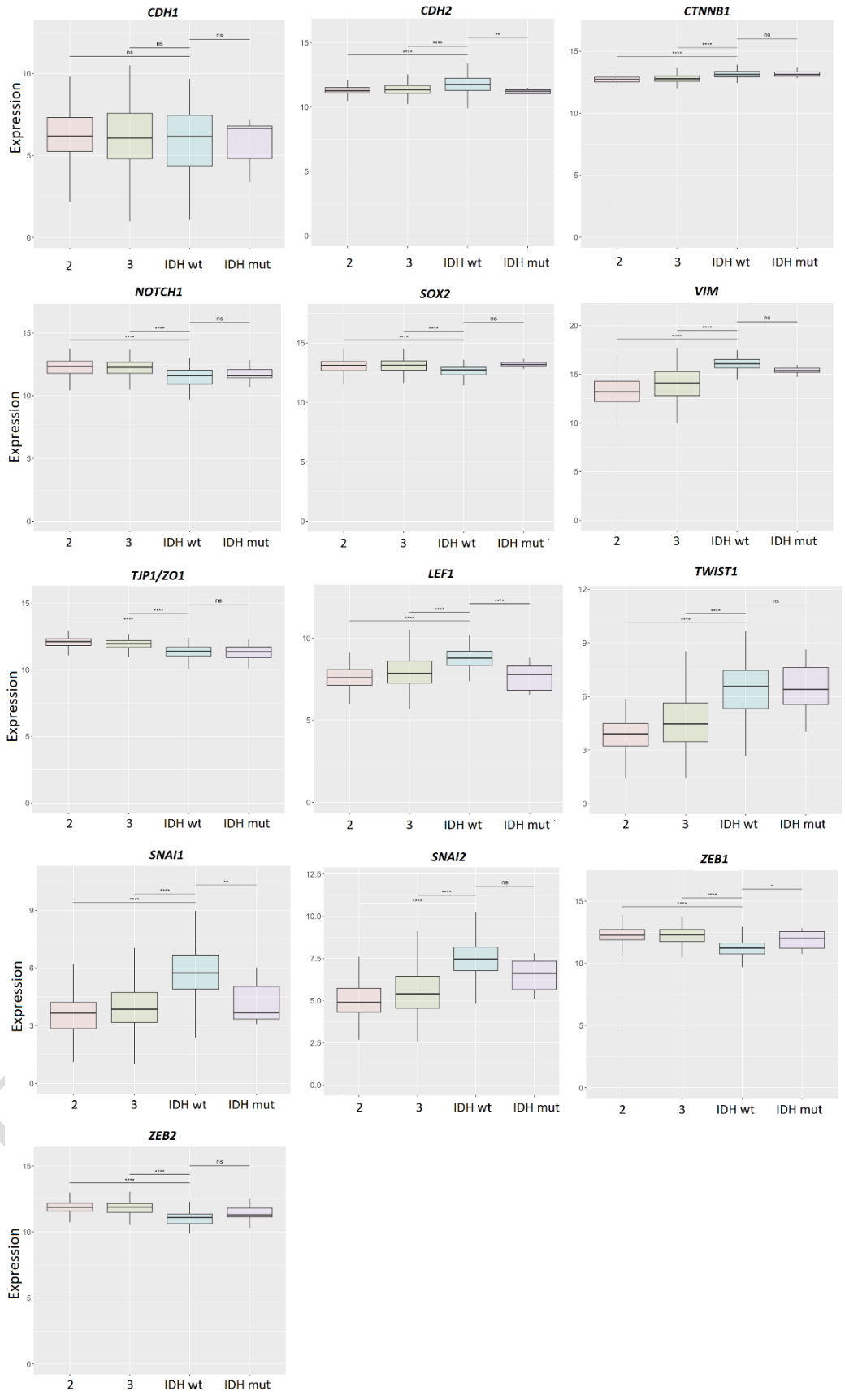
CDH1
CDH2
CTNNB1
NOTCH1
SOX2
VIM
TJP1/ZO1
LEF1
TWIST1
SNAI1
SNAI2
ZEB1
ZEB2
Expression
2
3
IDH wt
IDH mut

Figure 5. Differential expression stratified according to *IDH1* status. Results are presented as mean +/- SD. * $p<0.05$, ** $p<0.01$, *** $p<0.001$, *** $p<0.0001$ (one-way ANOVA with Tukey's post hoc test). 2, 3, IDH1wt (4), IDH1 mut (4) represent glioma grades.

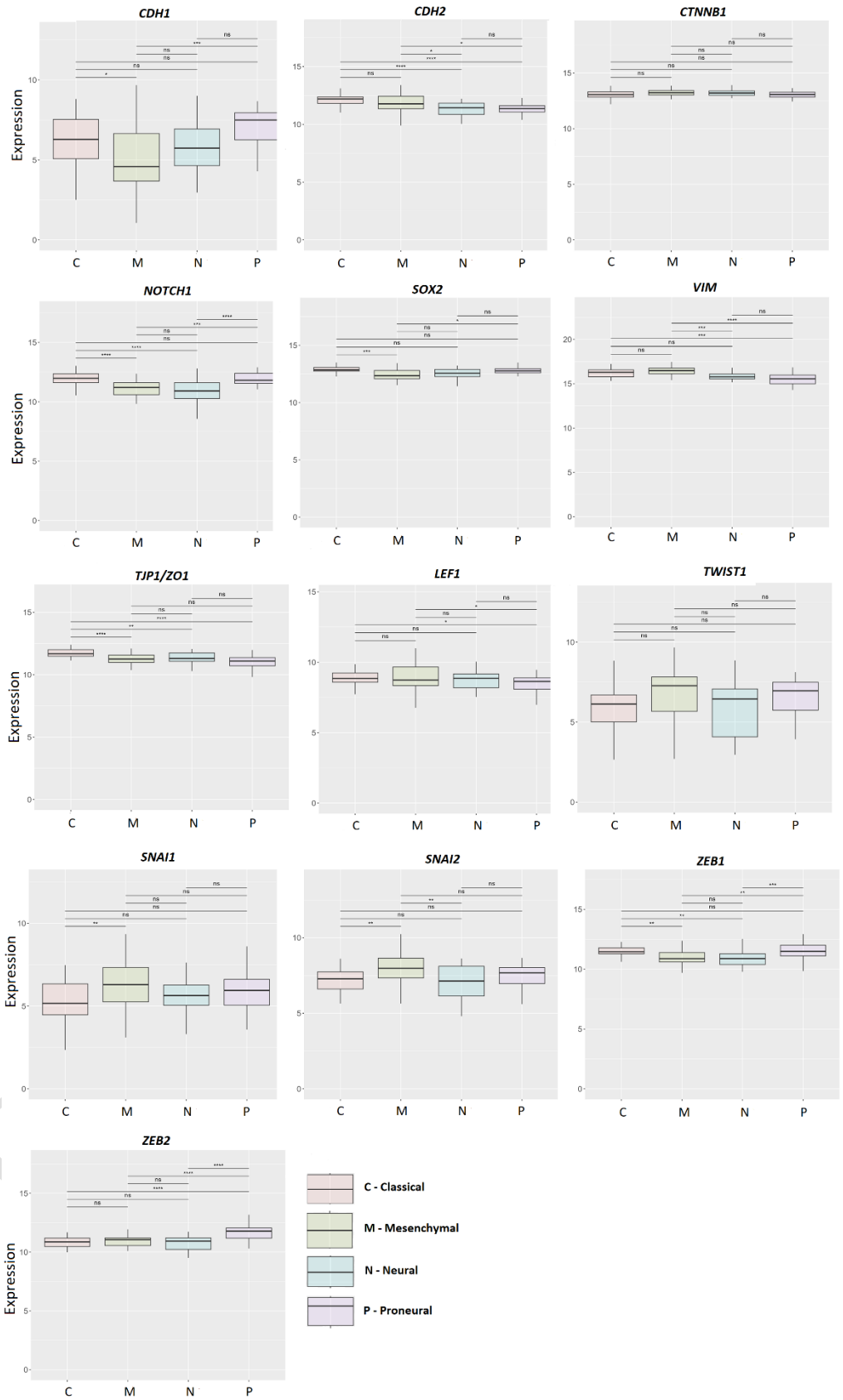
CDH1
CDH2
CTNNB1
NOTCH1
SOX2
VIM
TJP1/ZO1
LEF1
TWIST1
SNAI1
SNAI2
ZEB1
ZEB2
Expression
C
M
N
P
C - Classical
M - Mesenchymal
N - Neural
P - Proneural

Figure 6. Differential expression in grade 2, grade 3 and grade 4 (glioblastoma) stratified according to glioblastoma subtypes, classical, mesenchymal, proneural and neural. Results are presented as mean +/- SD. * $p<0.05$, ** $p<0.01$, *** $p<0.001$, *** $p<0.0001$ (one-way ANOVA with Tukey's post hoc test).

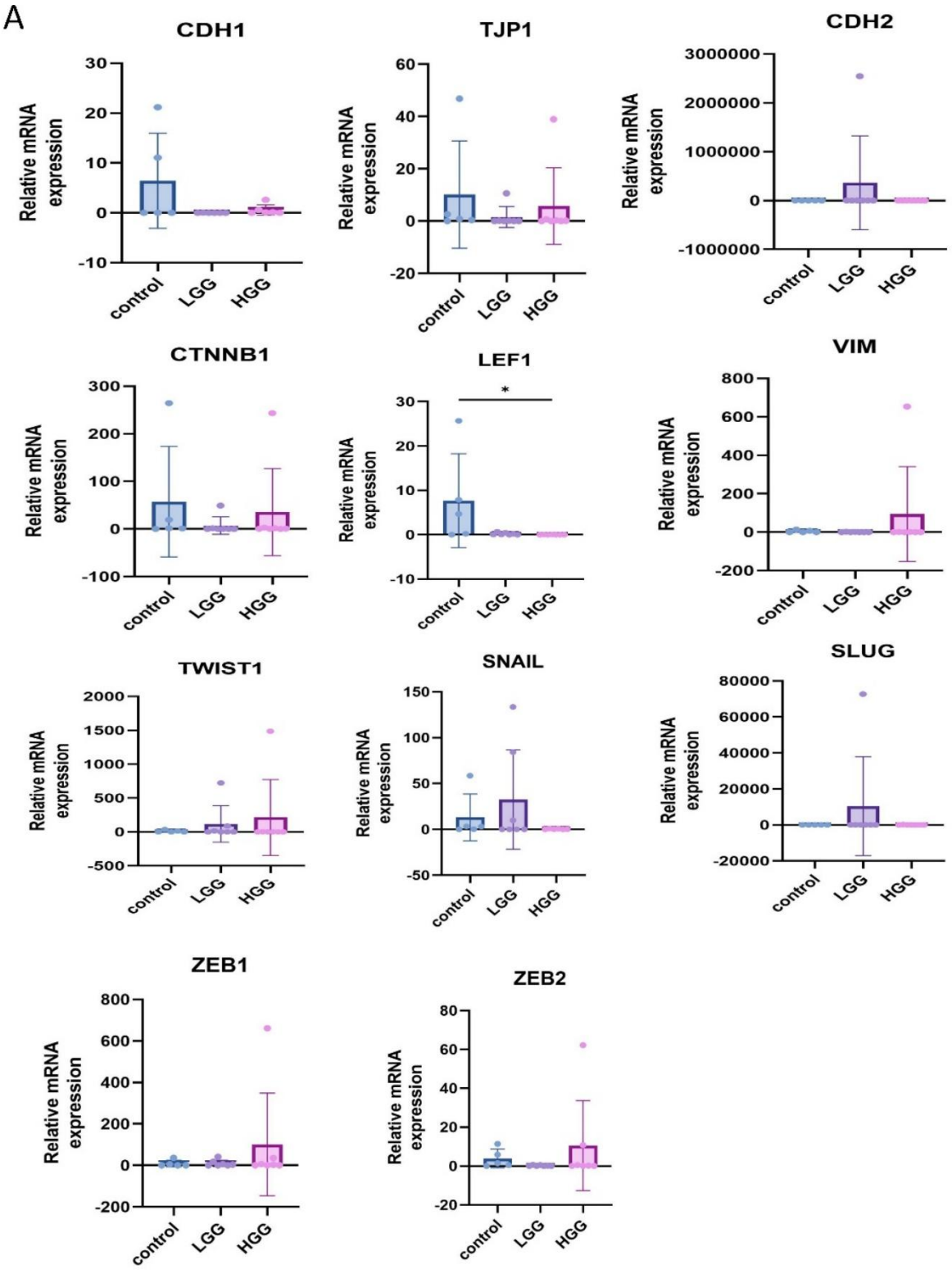
A
CDH1
TJP1
CDH2
CTNNB1
LEF1
VIM
TWIST1
SNAIL
SLUG
ZEB1
ZEB2
Relative mRNA expression
control
LGG
HGG
*

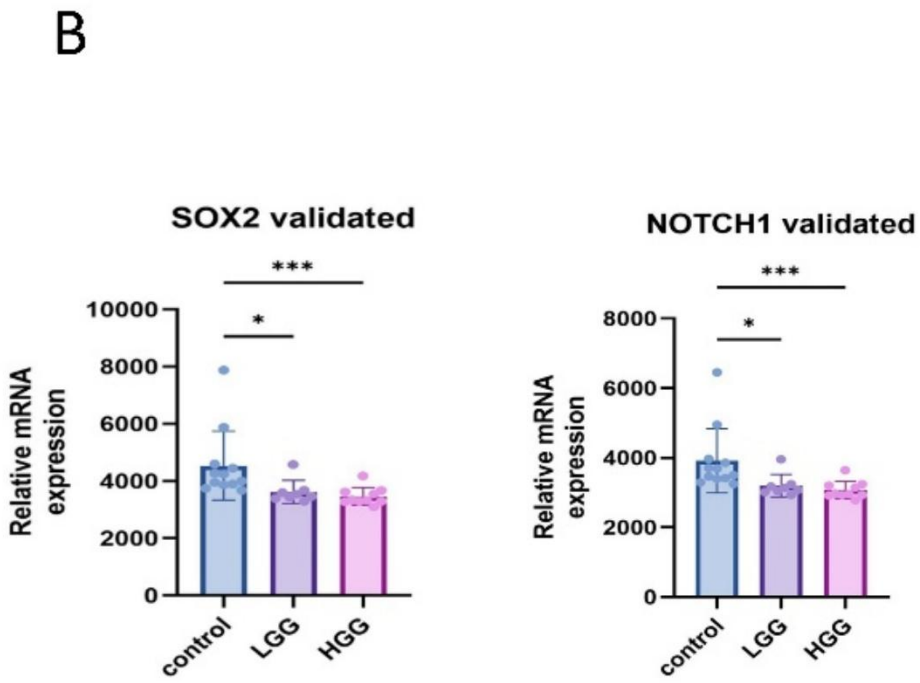

Figure 7.A. qRT-PCR of analyzed genes. B. qRT-PCR of *NOTCH1* and *SOX2* genes was validated on additional experiments. Results are presented as mean +/- SD. * $p<0.05$, ** $p<0.01$, *** $p<0.001$, *** $p<0.0001$.

A

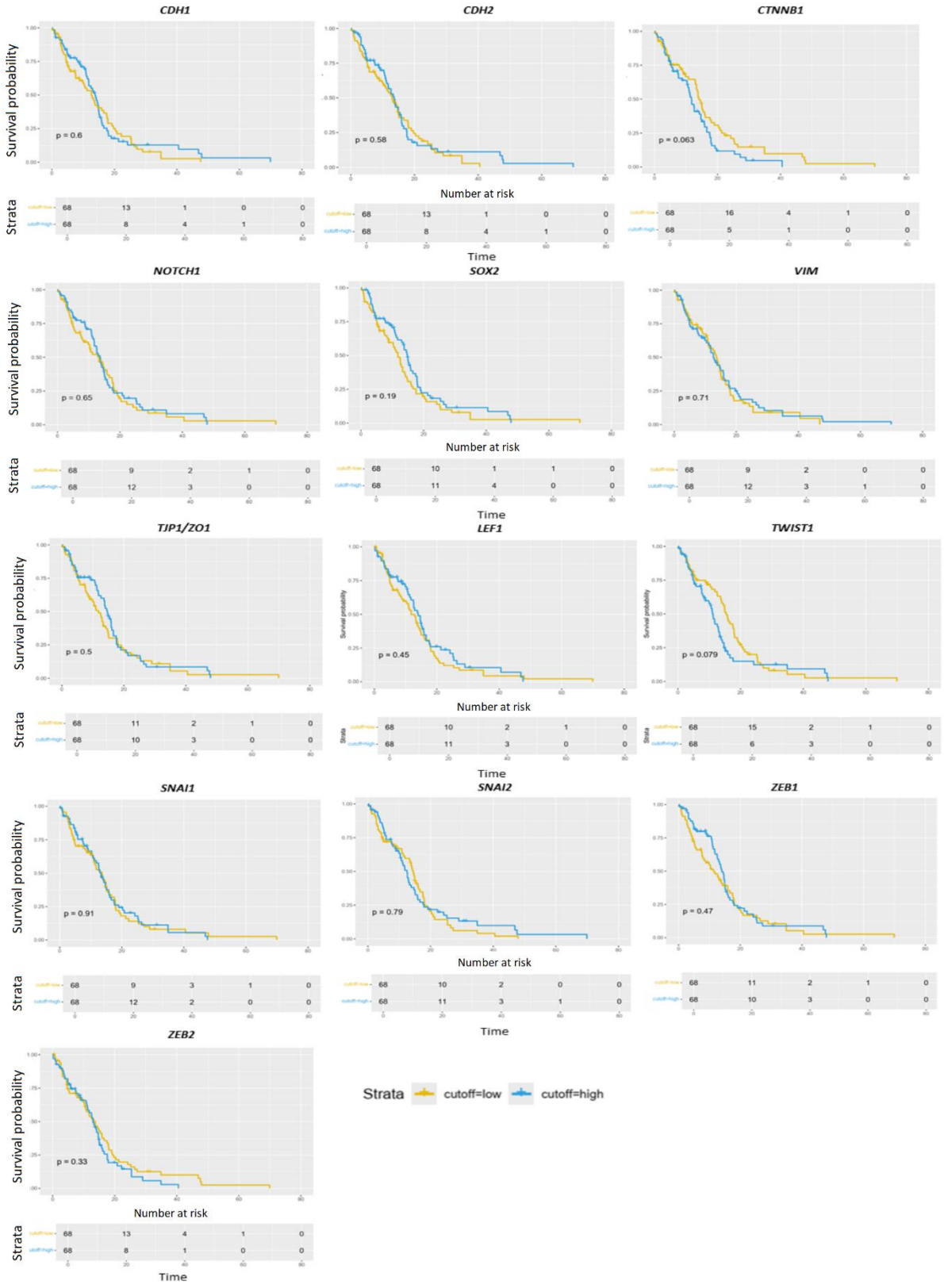
CDH1
p = 0.6
CDH2
p = 0.58
CTNNB1
p = 0.063
NOTCH1
p = 0.65
SOX2
p = 0.19
VIM
p = 0.71
TJP1/ZO1
p = 0.5
LEF1
p = 0.45
TWIST1
p = 0.079
SNAI1
p = 0.91
SNAI2
p = 0.79
ZEB1
p = 0.47
ZEB2
p = 0.33
Survival probability
Number at risk
Strata
Time
Strata cutoff=low cutoff=high

B

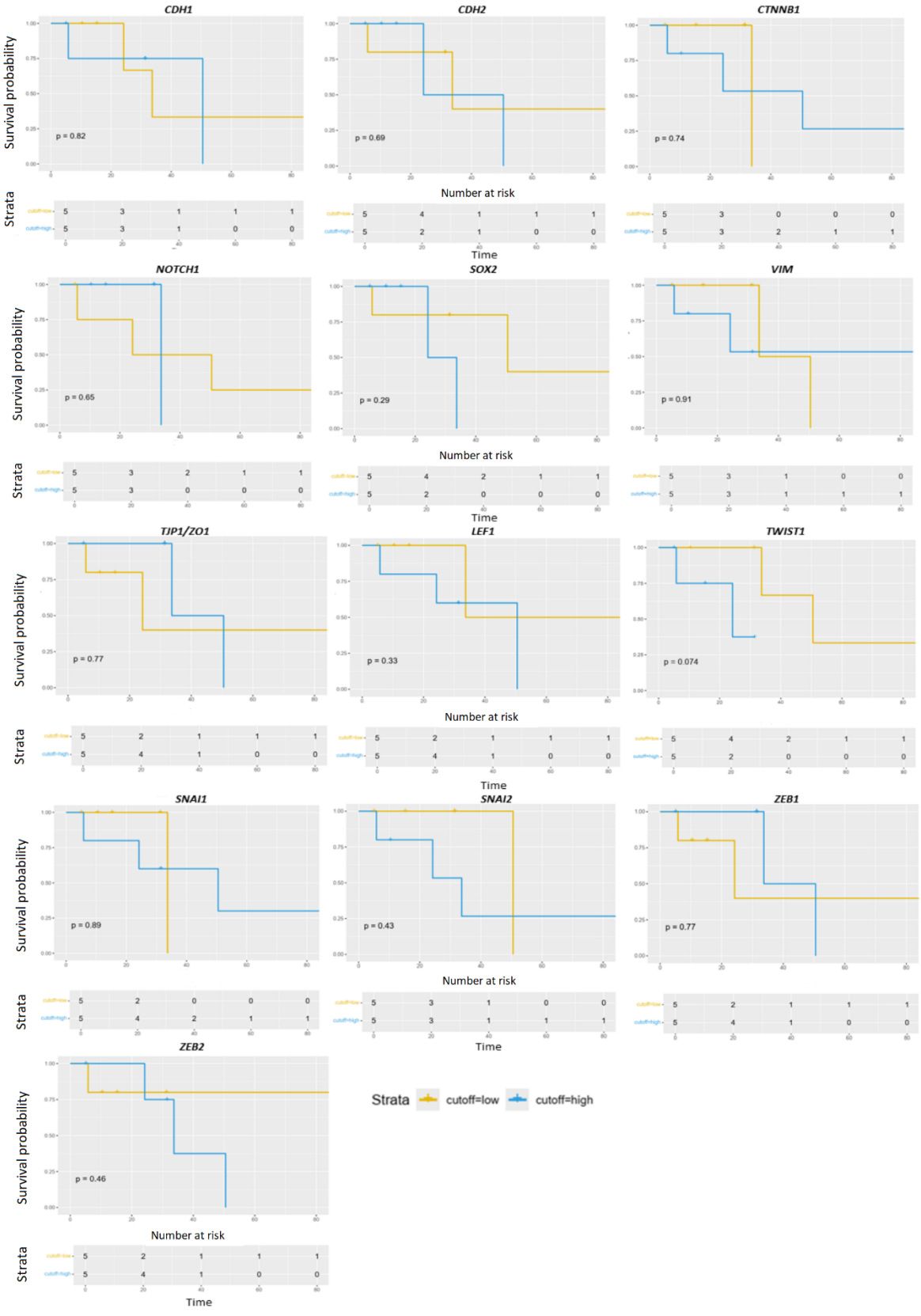
CDH1
CDH2
CTNNB1
NOTCH1
SOX2
VIM
TJP1/ZO1
LEF1
TWIST1
SNAI1
SNAI2
ZEB1
ZEB2
Survival probability
p = 0.82
p = 0.69
p = 0.74
p = 0.65
p = 0.29
p = 0.91
p = 0.77
p = 0.33
p = 0.074
p = 0.89
p = 0.43
p = 0.77
p = 0.46
Number at risk
Strata
Time
Strata cutoff=low cutoff=high

Figure 8. Age adjusted survival analysis of glioblastoma patients related to EMT-associated genes. Kaplan–Meier curves of overall survival (OS) of genes involved in EMT in TCGA-GBMLGGcohort data. A. Glioblastoma *IDH1* WT age adjusted survival. B. Glioblastoma *IDH1* MUT age adjusted survival.

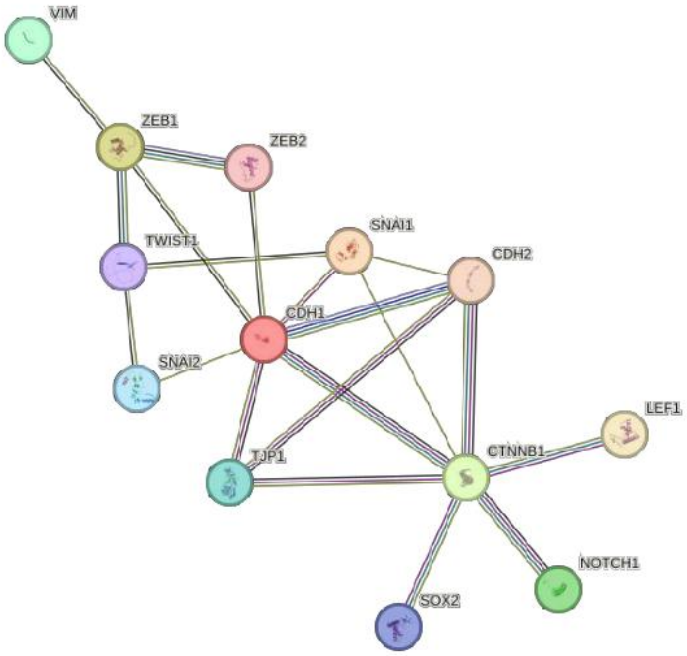

Figure 9. Protein network of EMT-related genes (STRING tool).

SUPPLEMENTAL DATA

Table S1. primer sequences used for qRT-PCR.

Gene	Forward primer	Reverse primer
ACTB	GAAGAGCTACGAGCTGCCTGA	CCACGTCACACTTCATGATGG
CDH1	GCCTCCTGAAAAGAGAGTGGAAG	TGGCAGTGTCTCTCCAAATCCG
	CCTCCAGAGTTTACTGCCATGAC	GTAGGATCTCCGCCACTGATTC
CTNNB1	CACAAGCAGAGTGCTGAAGGTG	GATTCCTGAGAGTCCAAAGACAG
LEF1	CTACCCATCCTCACTGTCAGTC	GGATGTTCCTGTTTGACCTGAGG
NOTCH1	GGTGAACTGCTCTGAGGAGATC	GGATTGCAGTCGTCCACGTTGA
SNAIL	TGCCCTCAAGATGCACATCCGA	GGGACAGGAGAAGGGCTTCTC
SLUG	ATCTGCGGCAAGGCGTTTTCCA	GAGCCCTCAGATTTGACCTGTC
SOX2	GCTACAGCATGATGCAGGACCA	TCTGCGAGCTGGTCATGGAGTT
TJP1/ZO-1	GTCCAGAATCTCGGAAAAGTGCC	CTTTCAGCGCACCATACCAACC
TWIST1	GCCAGGTACATCGACTTCCTCT	TCCATCCTCCAGACCGAGAAGG
VIM	AGGCAAAGCAGGAGTCCACTGA	ATCTGGCGTTCCAGGGACTCAT
ZEB1	GGCATACACCTACTCAACTACGG	TGGGCGGTGTAGAATCAGAGTC
ZEB2	AATGCACAGAGTGTGGCAAGGC	CTGCTGATGTGCGAACTGTAGG

Table S2. Crude qRT-PCR data.

Supplementary data are available at the following link:

https://www.bjbms.org/ojs/index.php/bjbms/article/view/12598/3958

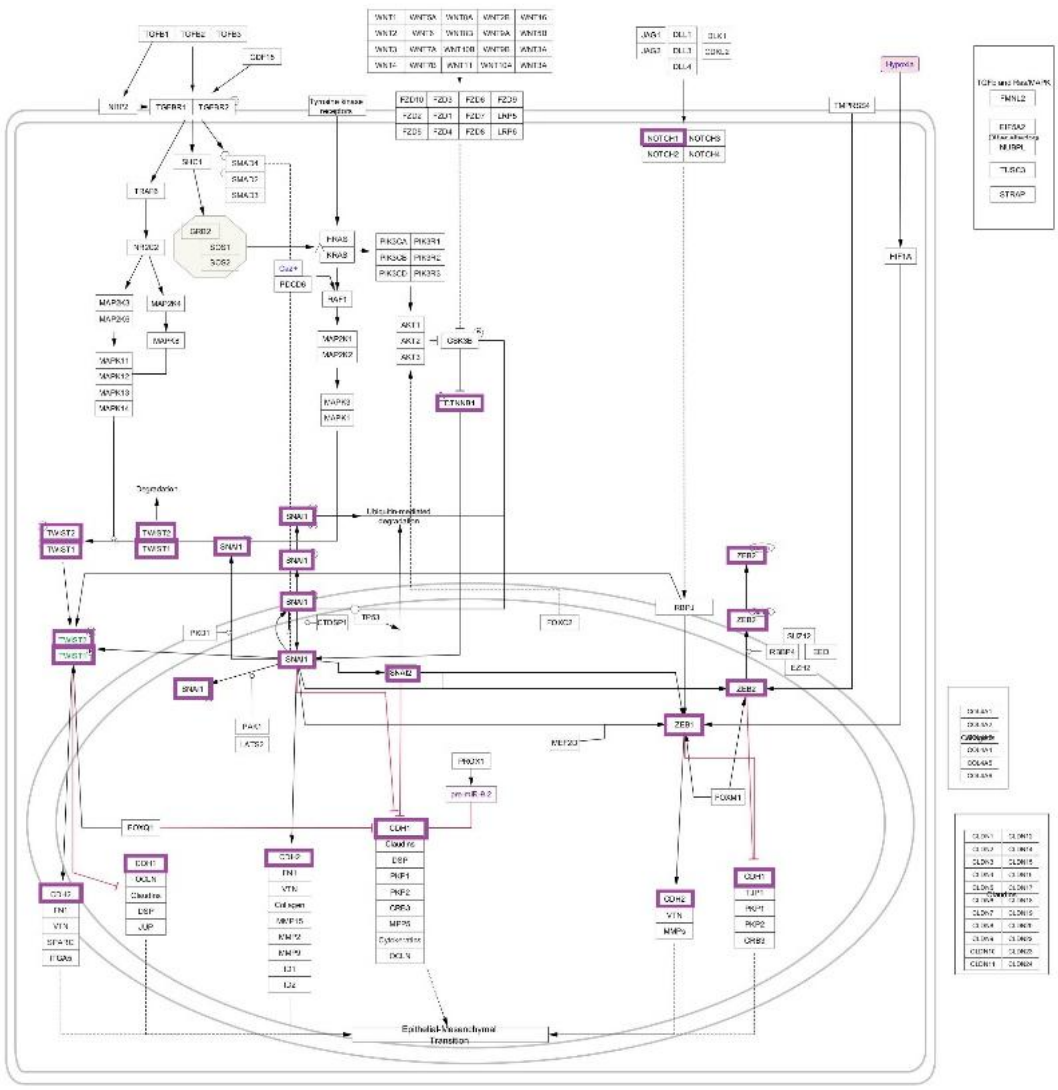

Figure S1. Pathway enrichment. Pathway WP4239 (Epithelial to mesenchymal transition in colorectal cancer) is presented.